Universidade do Porto

FEUP

Master in Biomedical Engineering

Heart Rate Variability Characterization Using Entropy Measures

Author: **Rebeca Goya Esteban**

Tutor: **Joaquim Pontes Marques de Sá**

Co-Tutor: **José Luis Rojo Álvarez**

June 1, 2008

Dissertation
Submitted to the
FEUP, Universidade do Porto
in Partial Fulfillment
of the Requirements for the Degree of
Master of Science in Biomedical Engineering.

Heart Rate Variability Characterization Using Entropy Measures

Rebeca Goya Esteban

Universidade do Porto
Faculdade de Engenharia
June 1, 2008

To my family.

If you really want something, and really work hard, and take advantage of opportunities, and never give up, you will find a way.

Jane Godall

Acknowledgments

First, I would like to thank Professors J.P. Marqués de Sá and J.L. Rojo Álvarez for guidance, support, freedom and helpful comments.

I especially thank Óscar, for everyday support, encouraging and stimulating theories, ideas and future plans.

I would also like to thank JL and Doctor Arcadio Garcia Alberola the opportunity of working in an amazing area and making so much easy to reconcile study and work. Thanks also to the rest of the "HRV team" from URJC ($\star$).

I would also like to thank the people from INEB Signal Processing Group for hosting us and making our stay in Portugal more genuine.

Finally, I would like to thank to my family for patience and support even in the distance.

Abstract

Heart Rate Variability (HRV), is defined as the variation in the interval between consecutive heart beats, or the variations between consecutive instantaneous heart rates, that occurs in the heart as a consequence of a complex internal dynamic balance. Since the state of the autonomic nervous system, and several related diseases, can be investigated noninvasively by the HRV, there exist a large number of indices used to characterize the condition of the cardiac system via the HRV signal.

Entropy based methods, present a good performance as irregularity measures as well as properties that make themselves suitable for physiological dataset analysis. They have been widely used for quantifying the HRV, with the hypothesis that decreasing entropy points to a perturbation of the complex physiological mechanisms or disease. However, higher entropy values have been reported in the literature for some pathologies than for healthy subjects, and there is not yet a clear consensus about the physiological meaning of these indices.

The aim of this work is to revise the nature of the HRV signal and the main methods used in its analysis, with special detail in the signal entropy-based methods, mainly, Approximate Entropy ($ApEn$), Sample Entropy ($SampEn$) and Multiscale Entropy (MSE). It is also the purpose of this work to study in details aspects such as the free parameters tuning of the algorithms, or the comparison between the methods performance.

These entropy methods are first studied in a controlled environment with well known synthetic signals. Then, the methods are tested on real signals from both healthy subjects and patients suffering from Congestive Heart Failure (CHF), with two main objectives: First, to quantify the discrimination capabilities of the methods between healthy and pathological subjects, and second, to asses the loss of HRV due to aging.

It is found that the use of a fixed threshold value r (free parameter of the algorithms), instead of the more widely popularized setting of r as a percentage of the standard deviation of each

data series, yields better discrimination between healthy and CHF subjects. It is also found that is possible to quantify the loss of HRV due to aging in healthy subjects which is not possible with variable threshold value r. Moreover, no correlation is found for CHF subjects between the age and the variation of the entropy results.

Therefore, it is concluded that the use of a fixed threshold value r in the algorithms, improves the discrimination capabilities between healthy and CHF subjects and also allows to quantify the loss of HRV due to aging in healthy subjects.

Resumo

A Variabilidade da Frequência Cardíaca (VFC), define-se como a variação do tempo entre batimentos cardíacos consecutivos, o as variações entre ritmos cardíacos istantaneos consecutivos que ocorrem no coração, como cosenquêcia de um complexo equilíbrio dinâmico interno. Dado que o estado do sistema nervoso autómo, e várias doenças relacionadas, podem ser investigadas de forma não invasiva por meio da VFC, existe um amplo conjunto de índices utilizados para avaliar a condição do sistema cardíaco através do sinal de VFC.

Os métodos baseados na entropía dos sinais, apresentam um bom desempenho como medidas de irregularidade, assim como um conjunto de propriedades adequadas para o análise de dados fisiológicos. Estes métodos têm sido ampliamente utilizados para a quantificação da VFC, com a hipótese de que valores decrescentes de entropia indicam alguma perturbação dos complexos mecanismos fisiológicos o algum tipo de doença. No entanto, na literatura têm sido relatados valores maiores de entropia para algumas patologias que para estados saudáveis, e ainda não existe um consenso claro sobre o significado fisiológico destes índices.

Neste trabalho apresenta-se uma revisão da natureza do sinal de VFC e dos principais métodos de análise do mesmo, com ênfase nos métodos baseados na entropia dos sinais, nomeadamente, a Entropia Aproximada (*ApEn*), a Entropia Amostral (*SampEn*) e a Entropia Multiescala (*MSE*). É também objectivo deste trabalho estudar em detalhe aspectos como o ajuste dos parámetros livres dos algoritmos ou a comparação entre o desempenho dos diferentes algoritmos.

Os métodos de entropia são primeiro analisados num entorno controlado com sinais sintéticos conhecidos. A seguir, os métodos são analisados com sinais reais de sujeitos saudveis e sujeitos com Insuficiência Cardíaca Congestiva (ICC) com dois objectivos principais: primeiro quantificar as capacidades de discriminação dos métodos entre os sujeitos saudáveis e os patológicos, e segundo, quantificar a perda da VFC devido à idade.

Face aos resultados encontra-se que o uso de um valor limiar r (parámetro livre dos algo-

ritmos) fixo , em lugar de um limiar dependente do desvio padrão de cada série temporal, que é a eleção mais ampliamente utilizada na literatura, consegue uma melhor discriminação entre sujeitos saudáveis e patológicos. Encontra-se também, que é possível quantificar a perda da VFC devida à idade em sujeitos saudáveis, enquanto que isto não é possível com um limiar r variável. Além disso, não se encontra correlação entre a idade e a variação dos valores de entropia para os sujeitos com ICC.

Portanto, conclue-se que o uso de um limiar fixo r nos algoritmos, melhora as capacidades discriminativas entre sujeitos saudáveis e sujeitos com ICC e permite a quantificação da perda da VFC devida à idade em sujeitos saudáveis.

Contents

List of Tables

List of Figures

Chapter 1

Introduction

According to World Health Organization (WHO), cardiovascular diseases are the first cause of death in the world, and it is expected to remain with that level of incidence during the next years. An estimated 17.5 million people died from cardiovascular disease in 2005, representing 30% of all global deaths. About 80% of these deaths occurred in low and middle-income countries. If current trends are allowed to continue, by 2015 an estimated 20 million people will die from cardiovascular disease [Organization 08].

The relationship between the autonomic nervous system and cardiovascular mortality has been recognized during the last decades, and it has motivated the development of quantitative markers of autonomic activity. Among them, the Heart Rate Variability (HRV), is defined as the variation in the interval between consecutive heart beats, that occurs in the heart as a consequence of a complex internal dynamic balance. Since this signal allows a noninvasive study of the state of the autonomic nervous system and of several related diseases, HRV has revealed itself as a powerful tool in the prognosis and diagnosis of a number of cardiovascular diseases [Malik 96].

Between the large number of indices that have been proposed to asses the HRV, signal entropy-based methods have been paid wide attention, first, for their good performance as irregularity measures, and second, because they present several properties that make themselves appropriate for physiological dataset analysis [Pincus 01]. However, although these methods have been widely applied in the last years with good results, in most works so far, the free parameters of the algorithms are set to values previously indicated in the literature, without studying systematically the impact they can have. The aim of this work is to study the influence

of the free parameters tuning in the assessment of the HRV loss due to aging, and in the characterization of the HRV of patients affected by Congestive Heart Failure (CHF), having in view a reliable discrimination between healthy and pathological subjects.

CHF, is a condition in which the heart cannot pump enough blood to the body organs. This can result from narrowed arteries that supply blood to the heart muscle, past heart attack or myocardial infarction, high blood pressure, heart valve disease, cardiomyopathies, congenital heart defects, or infection of the heart valves and/or heart muscle itself [Association 08]. With these pathologies, the heart can keep working but not as efficiently as it should. It has been shown that this condition affects to the HRV [Signorini 06, Costa 03a], and therefore, the analysis of the relationship between HRV and CHF is of clinical value.

The signal processing methods that are considered in this work, namely, the Approximate Entropy (*ApEn*), the Sample Entropy (*SampEn*) and the Multiscale Entropy (*MSE*), have been previously widely applied in several studies and in different fields [Pincus 01, Hornero 08]. One of these fields is the HRV analysis, they have been applied to the fetal heart rate signal (FHR) for the identification of fetal distress [Magenes 03, Ferrario 06], to the study of the sudden infant death syndrome(SIDS) [Pincus 01], to the characterization of FHR patterns to monitory fetus condition [Marques-de Sá 05], to the neonatal sepsis [Lake 02], to the discrimination between healthy dynamics and pathological dynamics [Costa 05], and to the distinction of arrhythmias [Schuckers 99].

In this work, the signal entropy methods are studied with two main objectives: First, to maximice the discrimination between healthy and pathological subjects, and second, to asses the loss of HRV due to aging, with the aim of building an aging curve of HRV loss for healthy subjects.

The structure of this work is as follows:

- In Chapter 2, a review of the main methods that have been proposed in the literature for the HRV analysis as well as an introduction to some basic concepts of the HRV signal are introduced and summarized.

- In Chapter 3, the entropy-based methods for the HRV signal analysis, namely, *ApEn*, *SampEn*, and *MSE*, are presented.

- In Chapter 4, first, a set of synthetic signals of different nature and known properties are presented. Following, several experiments are performed on this set of signals in order to

test the performance of the entropy methods introduced in Chapter 3. The dependence of the methods on their free parameters is tested in detail.

- In Chapter 5, the entropy methods are tested on real signals from both, healthy and CHF subjects, with two main objectives, first: To quantify the discrimination capabilities of the methods between healthy and pathological subjects, and second, to asses the loss of HRV due to aging.

- In Chapter 6, conclusions and further studies are presented.

Chapter 2

Heart Rate Variability

The study of the Heart Rate Variability (HRV) has revealed itself as a powerful tool in the prognosis and diagnosis of several cardiopathies. The relationship between the autonomic nervous system and cardiovascular mortality has been recognized in the last decades and has motivated the development of quantitative markers of autonomic activity, and among them, HRV is one of the most promising [Malik 96]. This chapter presents a review of the main methods for HRV analysis, as well as an introduction to some basic concepts on cardiac physiology.

2.1 Introduction

The heart behavior is not constant, but instead, there exists a variation of the time intervals between consecutive heart beats. The normal heart rhythm is controlled by the cardiac sinoatrial (SA) node, which is modulated by innervation from both the sympathetic and the vagal branches of the autonomic nervous system (ANS). The SA node is the final responsible, trough its repetitive nervous impulses, for generating heart beats.

Both the sympathetic and parasympathetic responses have antagonist roles, the activity from the sympathetic system increases the heart rate whereas the vagal activity slows down the heart rate. In rest conditions there is a balance state between these systems, that is responsible for the variability in the intervals between consecutive heart beats. At the same time, the ANS is influenced by many other systems (respiratory system, vasomotor system, central nervous system, renin-angiotensin system, ...) which also contribute to modulate the heart rate through it.

HRV is the variation in the intervals between consecutive heart beats, or, the variations between consecutive instantaneous heart rates. This signal allows noninvasive investigation of the ANS state and related diseases by the study of such variations. Therefore, the aim of studying HRV, is to extract the relevant clinical information underlying in it.

HRV has been proposed for risk stratification of lethal arrhythmias after acute myocardial infarction, as well as for the prognosis of sudden death events [Malik 96]. After a myocardial infarction, the innervation level of the heart decreases, and part of the nervous control of this organ can be lost. The HRV reflects this control loss and it makes possible the classification of cardiac sudden death risk groups [Malik 89]. The degeneration of the ANS due to the aging can also be inferred by the analysis of the HRV.

2.2 Electrocardiogram and Interval Tachogram

The electrocardiogram (ECG) is a graphic tracing produced by an electrocardiograph, which records the electrical activity of the heart over time. A typical ECG tracing of a normal cardiac cycle consists of a P wave, a QRS complex and a T wave. Also a small U wave is sometimes visible. The baseline voltage of the ECG is known as the isoelectric line. Each wave reflects a different stage of a heartbeat; their morphology and timing convey information that is used for diagnosing diseases that are reflected by disturbances of the heart electrical activity (Fig. 2.1). Atrial depolarization is reflected by the P wave, and ventricular depolarization is reflected by the QRS complex, whereas the T wave reflects ventricular repolarization. Atrial repolarization cannot usually be discerned from the ECG, since it coincides with the much larger QRS complex [Sörnmo 05].

The RR-intervals are defined as the distance between R-waves of consecutive beats[1]. The simplest graphical representation of the HRV is the tachogram (Fig 2.2), which represents the RR-interval durations versus the interval number.

If t_n is the occurrence time of the n-th R-wave, the interval tachogram $IT(n)$ is given by:

$$IT(n) = (t_n - t_{n-1}) \quad \text{for} \quad n = 1, ..., N. \tag{2.1}$$

[1]In some studies the nomenclature *NN-intervals* is used to denote that the ectopic beats (the ones that do not have their origin at the SA node) have been removed from the RR signal [Malik 96]. In this work just the sinusal beats are included in the computations, but the nomenclature *RR-intervals* is used to refer the signals

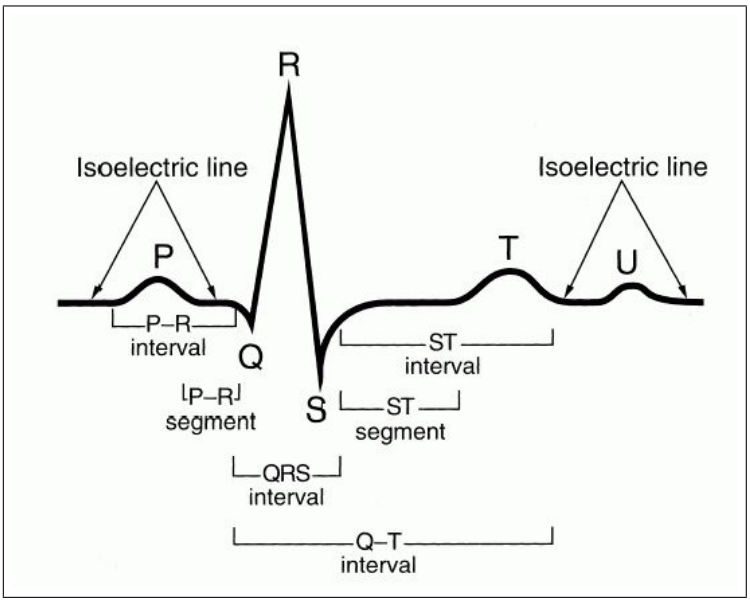

Figure 2.1: *The figure represents an ECG tracing diagram with the wave definitions (Taken from [Sauner 07]).*

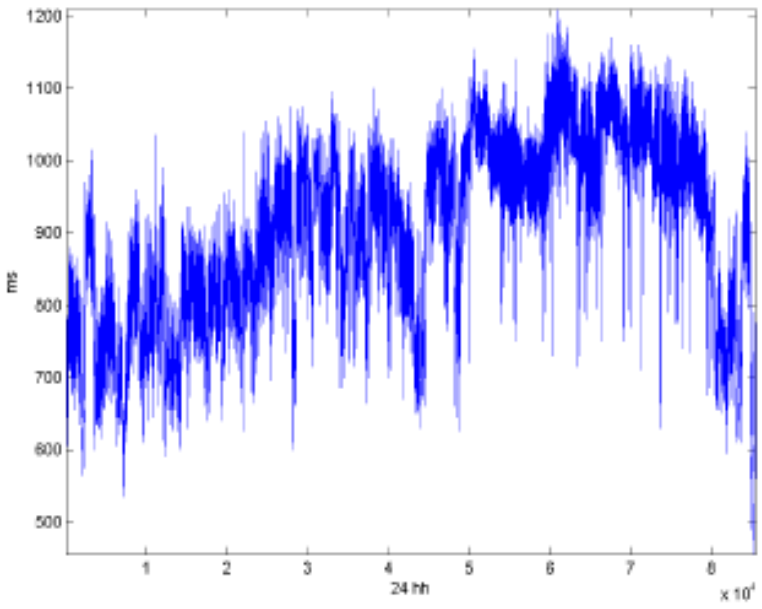

Figure 2.2: *Example of a tachogram from a patient, which represents the RR-interval durations versus the interval number.*

where N is the number of total intervals.

There exist several methods for RR-series analysis, each of them with different levels of complexity and with application in different contexts. In the following sections, the most relevant ones are described.

2.3 Linear Methods

Linear methods comprise time domain methods and spectral methods. Both have been used for decades, in several studies, to characterize HRV [O. Rompelman 77, Akselrod 81, Bigger 92, Piskorski 07]

2.3.1 Time Domain Methods

Time domain methods are the simplest ones on computational terms. They may be divided into statistical methods and geometric methods. Chronologically, they were the first to be applied to the HRV study, and they still are very used. Although a variety of heart rhythm representations may be used, the series of RR intervals is normally chosen for the design and calculation of time domain methods.

Statistical Indices

Statistical indices generally involve the calculation of the standard deviation or the variance of the RR-series [Malik 96, Mietus 02]. These may be divided into two classes:

1. Those derived from direct measurements of the RR intervals.

2. Those derived from the differences between RR intervals.

These indices may be derived from the analysis of long-term electrocardiographic recordings, usually 24 hour, or they may be calculated by using smaller segments of the recording period, usually 5 minutes. The latter approach allows comparison of HRV to be made during varying activities, e.g. sleep, awake activity, etc.

A subject to be taken into account is whether a particular index reflects long-term or short-term HRV, in order to know if the conveyed information is primarily related to parasympathetic

Index	Units	Description
AVNN	ms	Mean of NN intervals.
SDNN	ms	Standard deviation of NN intervals.
SDANN	ms	Standard deviation of the averages of NN intervals in all 5 min segments of the entire recording.
SDNNindex	ms	Mean of the standard deviations of NN intervals for all 5 min segments.
RMSSD	ms	The Square root of the mean of the sum of the squares of differences between adjacent NN intervals.
NN50		Number of pairs of adjacent NN intervals differing by more than 50 ms in the entire recording.
pNN50	%	NN50 divided by the total number of NN intervals.

Table 2.1: *Statistical indices of HRV*

or sympathetic activity [Sörnmo 05]. Indices obtained from the differences between RR intervals mostly convey short-term variability, due to the effect of the difference operation between consecutive samples.

Table 2.1 summarizes the most usual statistical indices.

Geometric Indices

Data analysis by statistical methods highly depend on the data quality. This quality may be affected by outliers, artifacts (noise generated by the measurement equipment), or even by the patient's cooperation capacity. Geometric methods come up from the search of more robust indices to face the lack of quality [Malik 96, Malik 89, Brennan 01, Piskorski 07].

Geometric indices derive from the geometric properties of the RR-series. These series can be represented as geometric patterns and then a simple formula is used to asses the variability based on the geometric or graphic properties of the resulting pattern. Three general approaches are used in geometric methods:

1. The HRV is obtained by a basic measurement of the geometric pattern, for example, the width of the distribution histogram at the specified level.

2. The geometric pattern is interpolated by a mathematically defined shape, for example, it could be the approximation of the distribution histogram by a triangle, or the approximation of the differential histogram by an exponential curve and then the HRV is measured from the parameters of the geometric shape.

3. The geometric shape is classified into several pattern-based categories, which represent different classes of HRV, for example, the elliptic, linear, and triangular shapes of Lorenz

Index	Units	Description
Triangular index	ms	Total number of all NN intervals divided by the maximum of the density function (height of the histogram of all NN intervals).
TINN	ms	Base width of the minimum square difference triangular interpolation of the highest peak of the histogram of all NN intervals
Lorenz plot dispersion	ms	Representation of each NN interval duration versus the duration of the previous interval.
Differential index	ms	Difference between the widths of the histogram of differences between adjacent NN intervals measured at selected heights.
Logarithmic index		Coefficient φ of the negative exponential curve $K \exp^{-\varphi t}$ which is the best approximation of the histogram of absolute differences between adjacent intervals.

Table 2.2: *Geometric indices of HRV.*

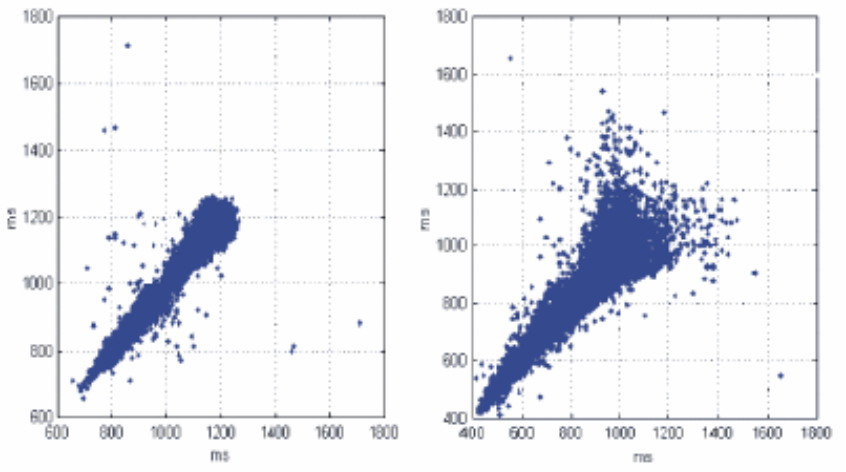

Figure 2.3: *Left represents a Lorenz plot with low scatter which means a low variability, while right shows a Lorenz plot with higher scatter which indicates therefore higher variability.*

plot, which is a graphical representation of each RR-interval duration versus the duration of the previous interval. Figure 2.3 shows an example of the Lorenz plot scatter.

Table 2.2 summarizes the most common geometric indices.

The application of geometric methods needs a reasonable number of RR intervals, preferably 24 hour, to build the geometric pattern, in order to ensure the correct performance of the methods.

2.3.2 Spectral Methods

Power spectral density (PSD) analysis provides the information of how power (variance) is distributed as a function of frequency.

Index	Units	Description
Total power	ms^2	Total variance of NN intervals over the temporal segment.
VLF	ms^2	Power in very low frequency range.
LF	ms^2	Power in low frequency range.
LF norm	u.n.	LF power in normalised units
		$LF/(\text{Total power} - VLF) * 100$.
HF	ms^2	Power in High frequency range.
HF norm	u.n.	HF power in normalised units
		$HF/(\text{Total power} - VLF) * 100$.
LF/HR		Ratio $LF[ms^2]/HF[ms^2]$.

Table 2.3: *Frequency domain Methods of HRV.*

HRV found in healthy subjects during rest is influenced by respiratory activity as well as by feedback mechanism of the systems for regulation of temperature and blood pressure. The different systems oscillate spontaneously at rest with characteristic frequencies in different intervals. By quantifying the power of the spectral components, information about pathologies related to cardiac autonomic function may be pointed out. The spectral domain is divided into different frequency intervals and then the spectral power is measured in each interval in associated with the physiologic response of the heart to the sympathetic or parasympathetic stimulation [Sörnmo 05, Bigger 92, Huikuri 99, Madera-Tejeda 02, Persson 97, Piskorski 07, Yan 95, Rojo-Álvarez 03].

Three main spectral components are distinguished in the PSD of the RR-series:

- Very low frequency band (VLF) [< 0.04] Hz.
- Low frequency band (LF) [0.04, 0.15] Hz.
- High frequency band (HF) [0.15, 0.4] Hz.

Frequency-domain measures listed in the Table 2.3 are calculated based on these spectral bands.

An increase in parasympathetic activity is related to an increase of the high-frequency power, whereas an increase in sympathetic activity is mainly related to an increase of the low-frequency power. However, is accepted that this last component has also influences from the parasympathetic brand [Cerutti 95]. The physiological explanation of the VLF component has not yet been established, and a specific physiological process ascribable to this component could be inexistent. Thus, VLF assessed from short-term recordings should be avoided when interpreting the PSD [Malik 96].

Spectral analysis of HRV signal is traditionally performed on stationary recordings of at least 256 to 512 consecutive heart beats, corresponding to a time window of a few minutes (2 - 5 min). This choice is made in order to obtain a good trade-off between a sufficient frequency resolution and the stationarity condition of the signal which is necessary for a reliable spectral estimation.

Methods for the calculation of PSD may be generally classified as non-parametric and parametric. Independently of the method employed, only an estimate of the true PSD of the signal can be obtained [Malik 96].

Non-parametric Methods

In non-parametric methods, the PSD estimation is obtained from the Fourier Transform of the Autocorrelation Function (ACF) of the signal. The Discrete Fourier Transform (DFT) can be quickly and efficiently obtained by the *Fast Fourier Transform* (FFT) algorithm. The expression of the PSD as a function of the frequency, can be obtained as:

$$P(e^{jw}) = \frac{1}{N\Delta t} \left| X(e^{jw}) \right|^2 \tag{2.2}$$

where Δt is the sampling period, N is the number of samples, and $X(e^{jw})$ is the DFT of the time series. This method is known as *Welch Periodogram* [Cerutti 95]. FFT based methods are widely used, for the simplicity of the algorithm employed and its high computational speed [Malik 96].

Parametric Methods

Parametric methods assume the time series under analysis to be the output of a linear system characterized by a rational function. In the parametric methods, the spectrum estimation procedure consists of two steps. Given the data sequence $y(n)$, with $y \leq n \leq N-1$, the parameters of the method are estimated. Then the PSD estimate is computed as a function of the model parameters [Guler 02].

An important point in this approach is the choice of an adequate model to represent the data sequence [Moody 06]. The most extended model is represented by the following linear equation that relates the input signal $\omega(k)$ and the output of an AutoRegresive p order process, AR(p):

$$y(k) = -\sum_{i=1}^{p} a_i y(k-1) + \omega(k) \tag{2.3}$$

where $\omega(k)$ is the input white gaussian noise and the a_i represent the model parameters. There exist two more parametric approaches, the AutoRegresive Moving Average model (ARMA) and the Moving Average model (MA). But since the estimation of the AR parameters results in linear equations, AR models, are the most widely used ones. Furthermore, an ARMA or MA process can be approximated by an AR model [Cerutti 95].

The AR PSD is then calculated from the following expression:

$$P(f) = \frac{\sigma^2 \Delta t}{|1 + \sum_{i=1}^{p} a_i z^{-i}|^2_{z=e^{(j2\Pi f_i \Delta t)}}} \tag{2.4}$$

Parametric methods are methodologically and computationally more complex than the non-parametric ones, as they require a priori choice of the model and its order. But they also have advantages, since they provide an accurate estimation of PSD even on a small number of samples, and they present smoother spectral components which can be easily distinguished, what makes easier the post-processing stage [Cerutti 95, Malik 96].

Figure 2.4 shows an example of the PSD calculation by parametric and non-parametric methods.

2.4 Non-linear Methods

Until now, we have assumed the signals we are dealing with, as the outputs of linear systems. However, it has been noticed that in normal conditions, fluctuations in the interval between consecutive heart beats may reveal characteristics from complex dynamic systems [Goldberger 91]. Based on this idea, conventional methods for the HRV signal analysis, might not extract all the information it conveys. This would make necessary to apply nonlinear appropriate tools [Goldberger 99, Barquero Pérez 05].

2.4.1 Methods from Chaos Theory

A nonlinear system can exhibit a very complex response. When the response of a nonlinear system has a strong sensitivity to initial conditions and it is difficult to predict, it is considered to have a chaotic behavior. An hypothesis in study, is that the complex heart rate fluctuations observed during normal sinus rhythm in healthy subjects are due in part to deterministic chaos and that a variety of pathologies, such as congestive heart failure syndromes, may involve a

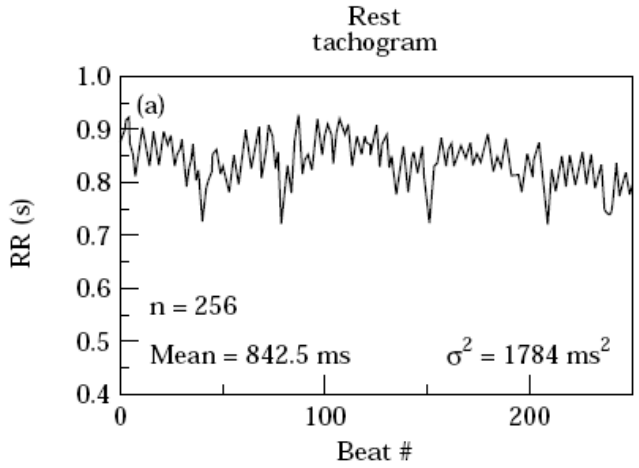

(a)

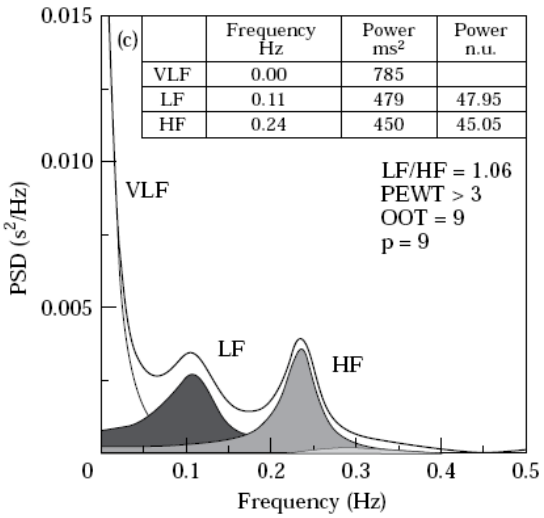

(b)

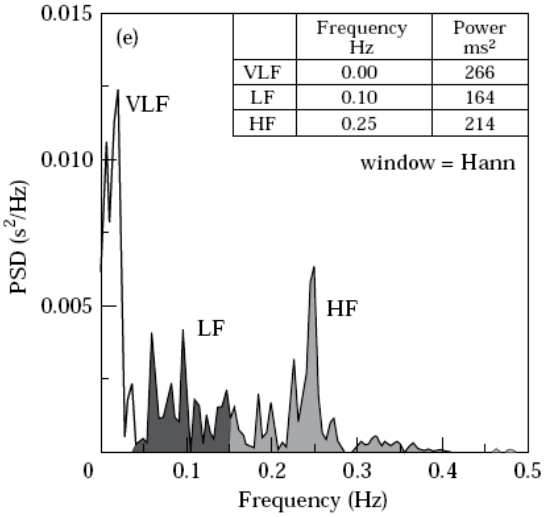

(c)

Figure 2.4: *PSD calculation. a)Tachogram of 256 consecutive RR values in a normal subject at supine rest, b)PSD calculation of the tachogram by parametric AR approach, c)PSD calculation of the tachogram by non-parametric approach (taken from [Malik 96]).*

paradoxical decrease in this type of nonlinear variability. The problem is that the mathematical algorithms designed for detecting chaos are not reliably applied to nonstationary data sets obtained from most clinical and physiological studies [Goldberger 99]. The most usual indices used to characterize these kind of system are:

- The correlation dimension, that measures the complexity of the dynamical systems by computing the fractal dimension of the system attractor, i.e., is a estimation of the degrees of freedom of the system [Lombardi 96].
- The Lyapunov exponents, that measures the dependence of the chaotic systems on the initial conditions [Signiorini 94].

2.4.2 Fractal Methods

The term fractal is a geometric concept, associated to forms that are highly irregular and have non-integer, dimensions. A fractal is an object composed of subunits that resemble the larger structure, this property is known as self-similarity. A number of cardiopulmonary structures have a fractal-like appearance (arterial and venous trees, the His-Purkinje network, etc.), but the fractality concept is not just applied to geometric forms, but also to complex processes that have more than a single time scale. Complex fluctuations with statistical properties of fractals have been described for HRV. Then, apparently health variability could be measured adapting quantitative tools derived from fractal mathematics [Goldberger 99]. Methods that allow the characterization of a complex system taking advantage of the fractal structure of the temporal series, generated by the own system are [Huikuri 00]:

- The $1/f$ slope, that is, the slope founded in the plot of the spectral power in bilogarithmic scale.
- The Hurst exponent.
- The scaling exponents from the Detrended Fluctuations Analysis (DFA).

2.4.3 Entropy Methods

Entropy-based methods provide a quantification of the irregularity of a temporal series. The entropy concept has to do with the uncertainty inherent on a signal, i.e., with the amount of

information it contains. The motivation to study the amount of irregularity or information in the HRV signal is based on the following idea: For different health states, signals with different irregularity levels are obtained, which means that it might be possible the stratification of risk groups for pathologies that affect to this characteristic. To study in depth the methods based in this concept and their performance is the purpose of the next chapters.

2.5 Conclusion

The methods presented in this chapter have different advantages and drawbacks. For this reason, their application depends on the circumstances of the study.

Statistical indices are the simplest ones in computational terms, but they are highly dependent on the data quality. Geometric indices come up to deal with this lack of quality and they are more robust, but there is a need of a reasonable number of RR intervals in order to ensure the correct performance of the these methods.

Sometimes, the spectral analysis contributes to understand better the mechanisms of the ANS and the fluctuations on the cardiac cycle. In order to perform these measures, the PSD estimation of HRV can be carried out either by parametric or by non-parametric methods. The first ones are methodologically and computationally more complex, but they achieve an accurate estimation of PSD even on a small number of samples.

More recently, it has been noticed that, in normal conditions, fluctuations in the interval between consecutive heart beats may reveal characteristics from complex dynamic systems. Therefore, non-linear approaches come up trying to extract all the information necessary to analyze the HRV signal that traditional methods cannot reveal.

The performance of these methods can be studied individually, over a set of signals, but often, several methods are computed in the same studies in order to compare them and also to obtain a deeper analysis of the signals.

Chapter 3

Entropy Methods

The presence of non-linear dynamics in physiological signals, makes necessary the application of adequate methods to this domain. Among the wide variety of proposed indices, methods based on the signal entropy calculation are an option that have arisen a wide interest during the last years.

The use of these methods to quantify data irregularity in cardiac signals is motivated by the meaningful differences founded with respect to the degree of irregularity on these signals depending on the health states, which reflects important physiological information.

3.1 Historical Development

Entropy is a thermodynamical quantity that describes the amount of disorder in a system. This concept was generalized to the characterization of information amount conveyed by probabilistic distributions. This topic is studied by the *Information Theory*, which was developed since 1940, major contributions belong to Shannon, Renyi and Kolmogorov. Information Theory has previously proved to be an appropriate approach to temporal series analysis [Kantz 04].

The Renyi entropies, a generalization of the Shannon entropy, are a family of functions that quantify the uncertainty or randomness in a system. The Renyi entropy of order q of a single discrete random variable X, with a set of values Θ and probability mass function $p(x_i) = P_r\{X = x_i\}$, where, $x_i \in \Theta$, is defined as

$$H_q(X) = \frac{1}{1-q} \ln \sum_{x_i \in \Theta} p(x_i)^q \tag{3.1}$$

and it is defined for all positive q except for $q = 1$.

The case where $q = 1$ can be evaluated by the l'Hôpital rule obtaining the Shannon entropy

$$H(X) = -\sum_{x_i \in \Theta} p(x_i) \ln p(x_i) \tag{3.2}$$

For a time series that represent the output of a stochastic process, that is, an indexed sequence of n random variables, $\{X_i\} = \{X_1, ..., X_n\}$, with a set of values $\theta_1, ..., \theta_n$, respectively, the joint entropy is defined as

$$H_n = H(X_1, X_2, ..., X_n) = -\sum_{x_1 \in \theta_1} ... \sum_{x_n \in \theta_n} p(x_1, ..., x_n) \ln p(x_1, ..., x_n) \tag{3.3}$$

where $p(x_1, ..., x_n) = P_r \{X_1 = x_1, ..., X_n = x_n\}$ is the joint probability for the n variables $X_1, ..., X_n$.

By using the chain rule in (3.3), the joint entropy, H_n, can be written as a summation of conditional entropies, $H(X_i|X_j)$ each of which is a non-negative quantity

$$H_n = \sum_{i=1}^{n} H\left(X_i|X_{i-1}, ...X_1\right) \tag{3.4}$$

Therefore, it can be concluded that the joint entropy is an increasing function of n. The rate at which the joint entropy grows can be written as

$$h = \lim_{n \to \infty} \frac{H_n}{n} \tag{3.5}$$

Let us now consider a D-dimensional dynamical system. Suppose that the phase space of the system is partitioned into hypercubes of volume ϵ^D, and that the state of the system is measured at time intervals δ. If $p(k_1, k_2, ..., k_n)$ denotes the joint probability that the state of the system is in the hypercube k_1 at $t = \delta$, in the k_2 at $t = 2\delta$, and in the k_n at $t = n\delta$, the Kolmogorov-Sinai (KS) entropy, H_{KS}, can be defined as

$$H_{KS} = -\lim_{\delta \to 0} \lim_{\epsilon \to 0} \lim_{n \to \infty} \frac{1}{n\delta} \sum_{k_1 ... k_n} p(k_1, ..., k_n) \ln p(k_1, ..., k_n) = \lim_{\delta \to 0} \lim_{\epsilon \to 0} \lim_{n \to \infty} \frac{1}{n\delta} H_n \tag{3.6}$$

For stationary processes [Cover 91], it can be shown that

$$\lim_{n \to \infty} \frac{H_n}{n} = \lim_{n \to \infty} H(X_n|X_{n-1}, ...X_1) \tag{3.7}$$

Then, by applying the chain rule, we obtain

$$H_{KS} = \lim_{\delta \to 0} \lim_{\epsilon \to 0} \lim_{n \to \infty} (H_{n+1} - H_n) \tag{3.8}$$

The state of a system at a certain instant t_i is partially determined by its history $t_1, t_2, ..., t_{i-1}$. However, each new state adds an additional amount of new information. The KS-entropy measures the mean rate of creation of information.

Numerically, only entropies of finite order n can be computed. As n becomes large with respect to the length of a given time series, entropy H_n is underestimated and decays toward zero. Therefore, Eq (3.8) is inappropriate to estimate the entropy of finite length time series.

Several formulas have been proposed as an attempt of estimating the KS-entropy with reasonable accuracy. Grassberger and Procaccia [Grassberger 83] suggested the characterization of chaotic signals by calculating the K_2 entropy, which is a lower bound of the KS-entropy.

Let $\{X_i\} = \{x_1, ..., x_i, ..., x_N\}$ represent a time series of length N. Consider the m-length vectors $\mathbf{u}_m(i) = \{x_i, x_{i+1}, ..., x_{i+m-1}\}$, $1 \leq i \leq N - m + 1$. Be $n_i^m(r)$ the number of vectors that satisfy $d\left[\mathbf{u}_m(i), \mathbf{u}_m(j)\right] \leq r$, where d is the euclidean distance. Then

$$C_i^m(r) = \frac{n_i^m(r)}{N - m + 1} \tag{3.9}$$

represents the probability that any vector $\mathbf{u}_m(j)$ is close to the vector $\mathbf{u}_m(i)$ within r, that is, the euclidean distance between the vectors is less or equal to r. The average of the C_i^m is given by

$$C^m(r) = \frac{1}{N - m + 1} \sum_{i=1}^{N-m+1} C_i^m(r) \tag{3.10}$$

represents the probability that any two vectors are within r of each other. Then, K_2 is defined as

$$K_2 = \lim_{N \to \infty} \lim_{m \to \infty} \lim_{r \to 0} -\ln \left[C^{m+1}(r) - C^m(r)\right] \tag{3.11}$$

Following the same nomenclature, Eckmann and Ruelle [Eckmann 85] defined the function

$$\phi^m(r) = \frac{1}{N - m + 1} \sum_{i=1}^{N-m+1} \ln C_i^m(r) \tag{3.12}$$

considering the distance between two vectors as the maximum absolute difference between their components

$$d\left[\mathbf{u}_m(i), \mathbf{u}_m(j)\right] = \max\left\{|x(i+k) - x(j+k)| : 0 \leq k \leq m-1\right\} \tag{3.13}$$

Eckmann and Ruelle also suggested the calculation of the the KS-entropy as follows

$$H_{ER} = \lim_{N\to\infty} \lim_{m\to\infty} \lim_{r\to 0} \left[\phi^m(r) - \phi^{m+1}(r)\right] \tag{3.14}$$

where $\phi^{m+1} - \phi^m$ represents the average of the natural logarithm of the conditional probability that sequences close to each other for m consecutive data points will still be close to each other for $m+1$ consecutive data points [Costa 05].

Although this equation has been useful in classifying low dimensional chaotic systems, it cannot be applied to experimental data, since the result is infinity for a process with superimposed noise of any magnitude. Also, ER-entropy does not distinguish some processes that appear to differ in complexity, e.g., ER-entropy for the MIX process (See 4.1.3) is infinity, for all $p \neq 0$ [Pincus 91].

For the analysis of short and noisy time series, Pincus formulated a family of statistics known as *Approximate Entropy*, that are described in the following section.

3.2 Approximate Entropy

The Approximate Entropy (*ApEn*) is a statistic inspired on the chaotic systems measures, that asses the irregularity of a time series. This entropic measure was first proposed by Pincus [Pincus 91], and it exhibits a good performance in the characterization of randomness even when the data sequences are not very long. *ApEn* has been tested to differentiate from systems with different degrees of complexity, and it has also been applied to the HRV characterization from both fetus and adults, as well as to other physiological signals in several studies [Schuckers 99, Pincus 01, Magenes 03, Marques-de Sá 05, Magalhães 06, Ferrario 06].

3.2.1 *ApEn* Calculation Algorithm

In order to compute the *ApEn*, the specification of two parameters is previously required : the embedded dimension m, that is, the length of the vectors to be compared, and a noise filter threshold r. Given N data points $u(1), u(2), ...u(N)$ of a signal, the parameter *ApEn(m,r)* is defined as follows:

1. Vector sequences $x(1), ..., x(N-m+1)$ are obtained, defined by $\mathbf{x}(i) = [u(i), ..., u(i+m-1)]$ for $i = 1, ..., N-m+1$.

2. The distance between vectors $\mathbf{x}(i)$ and $\mathbf{x}(j)$, $d[\mathbf{x}(i), \mathbf{x}(j)]$ is defined as the maximum difference, in module, between their respective scalar components, this is

$$d[\mathbf{x}(i), \mathbf{x}(j)] = \max_{k=1,...,m} (|u(i+k-1) - u(j+k-1)|) \tag{3.15}$$

3. Based in this distance, the next correlation measure is defined

$$C_i^m(r) = \frac{(\text{number of j} \leq N-m+1 \text{ such that } d[x(i), x(j)] \leq r)}{(N-m+1)} \tag{3.16}$$

where the numerator counts, for a given vector $x(i)$, the number of times that $d[x(i), x(j)] \leq r$ for $j = 1, ..., N-m+1$.

4. Next, the average of the natural logarithm of $C_i^m(r)$ is computed for all i:

$$\Phi^m(r) = \frac{1}{N-m+1} \sum_{i=1}^{N-m+1} ln\ C_i^m(r) \tag{3.17}$$

5. Finally, the *ApEn* is defined as:

$$ApEn\,(m,r) = \begin{cases} \lim\limits_{N\to\infty} & \left[\Phi^m(r) - \Phi^{m+1}(r)\right] \quad \text{for } m > 0 \\ \lim\limits_{N\to\infty} & \left[-\Phi^1(r)\right] \quad \text{for } m = 0 \end{cases} \tag{3.18}$$

But, since in practice N is a finite number, the statistical estimate is computed as:

$$ApEn(m,r,N) = \begin{cases} \Phi^m(r) - \Phi^{m+1}(r) & \text{for } m > 0 \\ -\Phi^1(r) & \text{for } m = 0 \end{cases} \tag{3.19}$$

ApEn quantifies the likelihood that runs of patterns that are close for m observations do not remain close on next incremental comparisons. Therefore, series with repetitive patterns will produce a small *ApEn* values, while less predictable series will produce a larger *ApEn* values.

Clinically, relatively low values of the HR *ApEn* could be related to some pathology [Pincus 92, Marques-de Sá 05].

Parameter Selection

Signal comparison by *ApEn* must be done with fixed parameters m and r.

The maximum value that the parameter m can have is given by the definition of a critical value, $m_{\text{crit}}(N) = \max(m : 2^{2^m} \leq N)$. The specification of $m_{\text{crit}}(N)$ is motivated by an application of the methods of Orstein and Weiss [Orstein 90] and is interpreted as a limit of gradation as a function of sequence length by indicating a maximal order consistent with a convergent entropy estimate [Pincus 96]. In the application to HRV signal analysis, it is advisable to fix m as 1, 2, or 3, the variation obtained in the results with these values is not very noticeable [Pincus 91, Marques-de Sá 05, Magalhães 06].

Regarding parameter r, Pincus recommends values between the 10% and 25% of the standar deviation of the data [Pincus 91, Pincus 94, Pincus 01], hence obtaining this way a scale invariant measurement. However, better results were achieved in other studies by choosing a fixed r (indepedent from each data series standar deviation) [Marques-de Sá 05, Magalhães 06], since the fact of setting the parameter r to a percentage of the standard deviation of the data could render the method sensitive to outliers.

Moreover, to eliminate most of the noise present in the data, r should be larger than the noise level.

Typically, the value used for the number of samples N, goes from 100 to 5000, however, in order to obtain reasonable estimates at least 30^m samples must be used [Pincus 96].

ApEn Example

In the following example two signals of different nature are studied. These signals are, a deterministic periodic signal, specifically a sinusoidal signal, and the output of a nonlinear dynamic system, a signal based in the series x_n that follows the rule $x_o = 0.1$ e $x_{n+1} = 1 - 2x_n^2$, known as Ulam's map.

Figure 3.1 shows the temporal representation of both signals.

The *ApEn* values for both signals were computed and the obtained values (Table 3.1) confirm that the periodic signal is very regular, and therefore it has a very small *ApEn* value, while the nonlinear signal has a considerably larger *ApEn* value. The first column on the table shows the *ApEn* obtained directly from each signal. In the second column, for a better comparison of the *ApEn* values, a normalization has been done. To carry out the normalization, each value in the original signals has been mapped into 10 unique entire values, in order to construct an alphabet of 10 symbols. Then, the *ApEn* is computed upon the mapped new series and the obtained

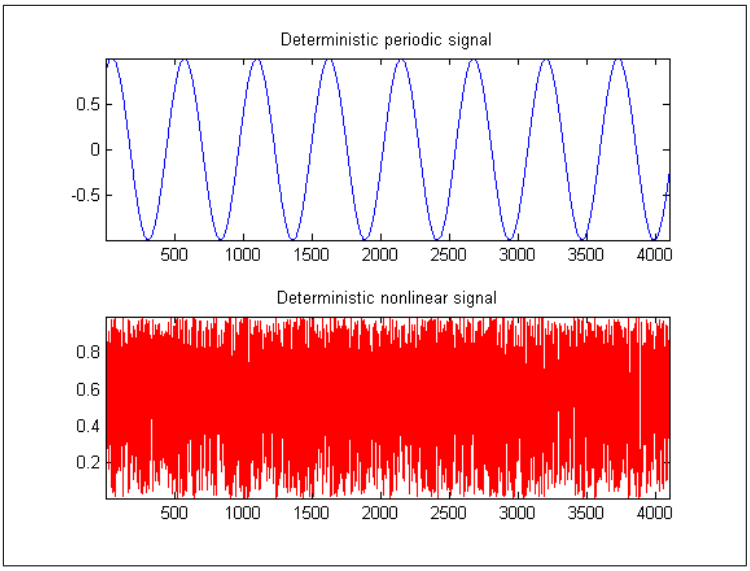

Figure 3.1: *Temporal representation of a deterministic periodic signal (top), and a deterministic nonlinear signal (bottom).*

Signal	***ApEn***	**Norm. *ApEn***
Deterministic periodic	0.0300	0.0695
Deterministic nonlinear	0.6493	0.3422

Table 3.1: *The table presents the ApEn values and also the normalized ApEn values for a deterministic periodic signal and for a deterministic nonlinear signal.*

values are normalized dividing by $ln(10)$ which is asymptotically the maximum value the *ApEn* can arise in series consisted of 10 symbols. This way, the maximum value of the *ApEn* after normalization is 1.

In this example, the difference between the irregularity of both signals is visually noticeable, but in other cases it can be not so evident, e.g. , in real signals from healthy and pathological subjects. Furthermore, since is not efficient to analyze visually all the signals in the studies and works, the quantification of the signals irregularity in order to compare a large amount of different registers seems useful.

3.2.2 *ApEn* Properties

Several properties of the *ApEn* make this statistic appropriate for physiological data set analysis [Pincus 01]:

- There is no need of a large amount of samples to obtain reasonable estimates.

- It is robust to outliers.
- It is nearly unaffected by the noise of magnitude below r.
- Increasing $ApEn$ corresponds to intuitively increasing process complexity.
- Its application is possible for stochastic, deterministic, and mixed processes, because finite values are obtained for all cases.

From these characteristics, the three first ones make the $ApEn$ appropriate to noisy short data series analysis. The last characteristic is adequate for the study of biological signals, since the outputs from biological systems usually have both, deterministic and random components.

In spite of the good properties for the characterization of physiological data exhibited by the $ApEn$, it also has some drawbacks:

- $ApEn$ is a biased statistic, due to the comparison of each template vector with itself to avoid the occurrence of $ln(0)$ in the algorithm. In the definition of $C_i^m(r)$, in the $ApEn$ computation, template vector $\mathbf{x}(i)$ itself counts in the $C_i^m(r)$ aggregation of vectors close to $\mathbf{x}(i)$. This has the consequence that the conditional probabilities in Eq. (3.19) are underestimated. This bias makes $ApEn$ dependent of the data length and uniformly lower than expected. For fixed m and r, the effect of this bias component tends to 0 as $N \to \infty$ [Pincus 94, Richman 00].
- $ApEn$ lacks relative consistency, it is expected that for most processes, if one process, U, exhibits more regularity than other, V, for one pair of parameters m and r, it is expected to do so for all other pairs, that is, if $ApEn(m1, r1)(U) \leq ApEn(m1, r1)(V)$, then $ApEn(m2, r2)(U) \leq ApEn(m2, r2)(V)$ [Richman 00]. The relative consistency does not hold for $ApEn$ statistic, as it will be outlined in the next chapter.

3.3 Sample Entropy

Trying to improve the algorithm face the problems exhibited by the $ApEn$, J.S Richman and J.R Moorman developed the family of statistics Sample Entropy ($SampEn$) [Richman 00, Lake 02], whose main differences relative to $ApEn$ are the followings:

1. It does not perform comparisons of each template vector with itself in its algorithm, that is, it does not count self-matches.

2. Just the first $N-m$ template vectors of length m are considered in both stages of the calculation, where $\Phi^m(r)$ and $\Phi^{m+1}(r)$ are computed respectively, while *ApEn* uses $N-m+1$ length vectors on the first step, to obtain $\Phi^m(r)$ and $N-m$ length vectors on the second step, to obtain $\Phi^{m+1}(r)$.

3. It does not use a template approach when estimating conditional probabilities, and hence, the probability measurement is directly obtained as the natural logarithm of the conditional probability instead of as the ratio of the logarithmic sums (see Eqs (3.17),(3.22)).

The *SampEn* is the negative natural logarithm of the conditional probability that two sequences similar for m points remain similar for *m+1* points, where self-matches are not included in calculating the probability. Thus, a lower value of *SampEn* also indicates more self-similarity in the time series. To be defined, *SampEn* requires only that two templates similar for m samples remain similar for *m+1* samples.

3.3.1 *SampEn* Calculation Algorithm

For the *SampEn* calculation the same parameters defined for the *ApEn* m and r are required. The *SampEn* algorithm is computed in the following steps:

1. $B_i^m(r)$ is defined as $(N-m-1)^{-1}$ times the number of template vectors $\mathbf{x}_m(j)$ similar to $\mathbf{x}_m(i)$ (within r) where $j = 1...N-m$ with $j \neq i$.

2. The average of $B_i^m(r)$ for all i is calculated as

$$B^m(r) = \frac{1}{N-m} \sum_{i=1}^{N-m} B_i^m(r) \tag{3.20}$$

3. Similarly $A_i^m(r)$ is defined as $(N-m-1)^{-1}$ times the number of template vectors $\mathbf{x}_{m+1}(j)$ similar to $\mathbf{x}_{m+1}(i)$ (within r) where $j = 1...N-m$ with $j \neq i$.

4. The average of $A_i^m(r)$ for all i is calculated as

$$A^m(r) = \frac{1}{N-m} \sum_{i=1}^{N-m} A_i^m(r) \tag{3.21}$$

$B^m(r)$ is then the probability that two sequences will match for m points, whereas $A^m(r)$ is the probability that two sequences will match for *m+1* points.

5. *SampEn(m,r)* is defined as follows

$$SampEn(m,r) = \lim_{N\to\infty} \{-\ln [A^m(r)/B^m(r)]\} \tag{3.22}$$

6. Which is estimated by the statistic *SampEn(m,r,N)*

$$SampEn(m,r,N) = -\ln [A^m(r)/B^m(r)] \tag{3.23}$$

7. If the total number of template matches of length m is called B,

$$B = \{[(N-m-1)(N-m)/2]\} B^m(r) \tag{3.24}$$

and the total number of template matches of length $m+1$ is called A,

$$A = \{[(N-m-1)(N-m)/2]\} A^m(r) \tag{3.25}$$

8. Replacing A and B in (3.23), we obtain

$$SampEn(m,r,N) = -\ln (A/B) \tag{3.26}$$

***SampEn* Example**

Figure 3.2 illustrates a situation where *SampEn* fulfills the relative consistency, but *ApEn* does not. For this example two processes with different known irregularity degree are chosen, *MIX(0.1)* and *MIX(0.9)* (See 4.1.3), both plotted in 3.2 (a). Notice that graphically, to maintain the relative consistency, plots of *ApEn* as a function of r for different data sets should not cross one another 3.2 (b). However, given that *MIX* processes have standard deviation of 1 approximately, it is observed, that *ApEn* keeps relative consistency over the statistically valid range of r.

3.3.2 *SampEn* Properties

In addition to maintain the original features that make *ApEn* appropriate for the study of physiological signals,

- *SampEn* achieves a bias reduction and turns itself less dependent of the data length.

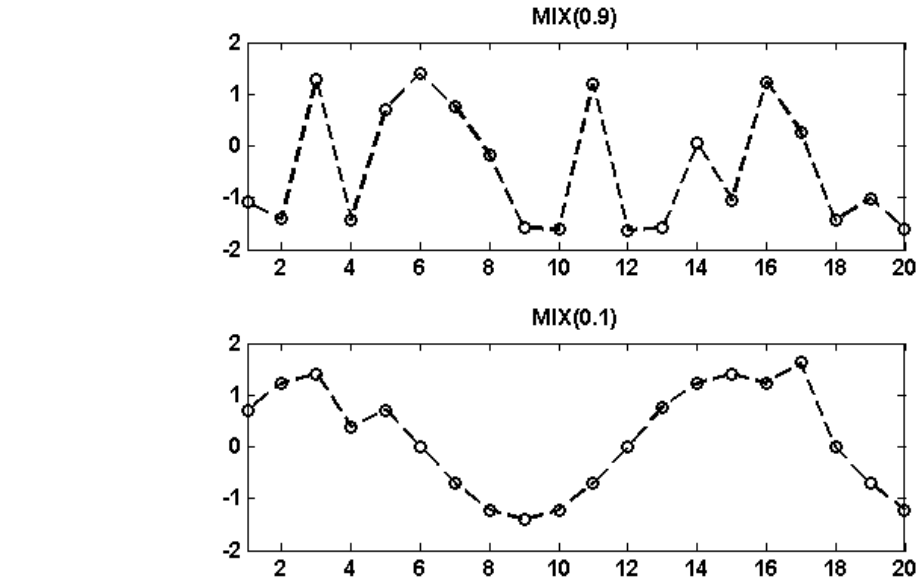

(a)

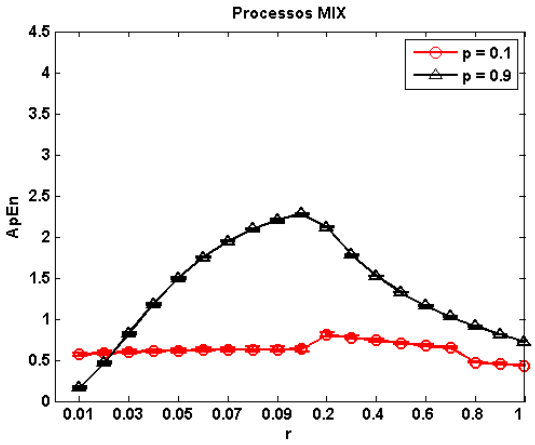

(b)

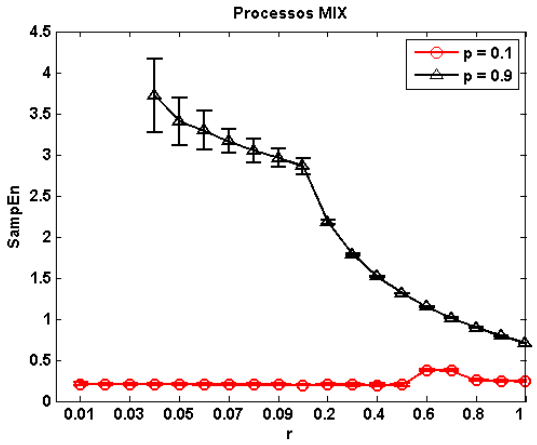

(c)

Figure 3.2: *a)20 samples of MIX(0.9) and MIX(0.1) processes are represented, the former with higher degree of irregularity than the last, b) ApEn statistics as a function of r with m=2 and N=5000, for MIX(0.9) and MIX(0.1), c)SampEn statistics as a function of r with m=2 and N=5000, for MIX(0.9) and MIX(0.1).*

- It presents relative consistency under circumstances where *ApEn* does not, although it cannot be assured that the *SampEn* presents the mentioned relative consistency for all time series. In essence, *SampEn* is an event counting statistic, where the events are instances of vectors being similar to one another. When the events are sparse, the statistics are expected to be unstable, which might lead to a lack of relative consistency.

3.4 Multiscale Entropy

Traditional entropy-based algorithms quantify the regularity of a time series. Entropy increases with the degree of irregularity and is maximum for completely random systems. However, an increase in the entropy may not always be associated with an increase in complexity.

Many pathologies, when associated with a more regular behavior, yield reduced entropy values in the physiological data, when compared to the healthy states. However, some pathologies, like atrial fibrillation, are associated with highly erratic fluctuations with statistical properties resembling uncorrelated noise. Traditional algorithms could yield higher entropies for such noisy pathological signals when compared to healthy dynamics, even though the latter represent more physiologically complex states.

This possible inconsistency may be due to the fact that traditional entropy algorithms are based on single scale analysis, and they could not take into account the complex temporal fluctuations inherent to healthy physiologic control systems.

The Multiscale entropy (*MSE*) suggests the analysis of the physiological time series in its different temporal scales [Costa 03a, Costa 03b, Costa 05]. The algorithm is inspired on Zhang's proposal of taking into account the information conveyed in multiple time scales [Zhang 91], but while in his work Zhang uses Shannon definition of entropy, which cannot be applied to physiological data series since it requires a large quantity of noise free data, the *MSE* uses *ApEn* or *SampEn* as entropy measures.

3.4.1 Calculation Algorithm

Given a discrete time series $x_1, ..., x_i, ..., x_N$, consecutive coarse-grained time series are obtained, $\left\{y^{(\tau)}\right\}$, determined by the scale factor τ.

- First, the original time series is divided in non-overlapping windows of length τ. Then, the average of the samples in each window is obtained. Figure 3.3 represents an example

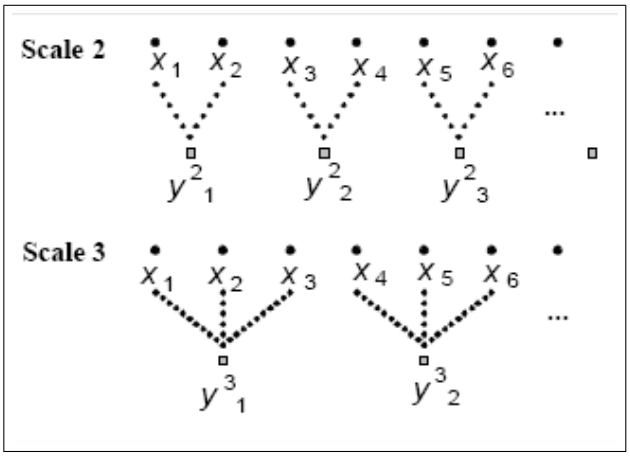

Figure 3.3: *Coarse-graining procedure for scales 2 and 3 (Taken from [Costa 03b]).*

of the construction of the coarse-grained temporal series for two scales.

- Each element of the coarse-grained time series $y_j^{(\tau)}$ is calculated according to the equation

$$y_j^{(\tau)} = 1/\tau \sum_{i=(j-1)\tau+1}^{j\tau} x_i, \quad 1 \leq j \leq N/\tau \tag{3.27}$$

  For scale one, time series $\{y^1\}$ is just the original time series.

  The length of each coarse-grained time series is equal to the length the original time series divided by the scale factor τ.

- Finally, the entropy index is calculated for each coarse-grained time series and plotted as a function of the scale factor τ.

The *MSE* method requires an adequate data length to obtain reliable statistics for each scale. Typically series of 2×10^4 have been used for analysis in 20 scales, in order to have at least 1×10^3 samples in the last coarse-grained series [Costa 05].

MSE Example

Figure 3.4 shows an example of the *MSE* method. *MSE* analysis of RR time series derived from 24 hour recordings of healthy young people, healthy elderly subjects and subjects with Congestive Heart Failure (CHF) is performed. In Figure 3.4 (a), an example of each time series is shown, and in Figure 3.4 (b) the result of the *MSE* analysis is presented. For scale one, which is the only scale considered by single-scale-based methods, the entropy assigned to the

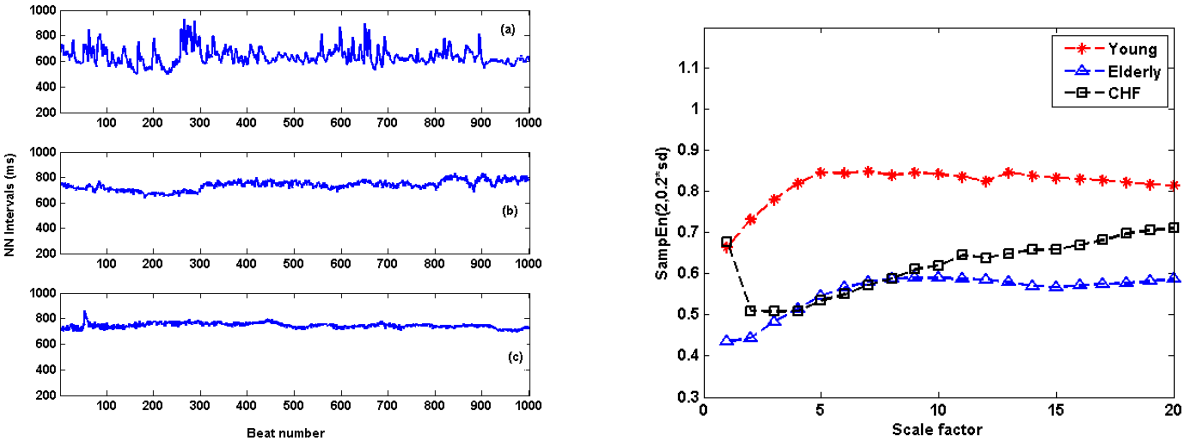

Figure 3.4: *The figure represents MSE analysis of RR time series derived from 24 hour recordings of healthy young people, healthy elderly subjects and Congestive Heart Failure subjects (CHF). (A) Interbeat interval series from: a)healthy young subject, b)healthy elderly subject, c) subject with CHF. (B) MSE analysis of the series. Symbols represent mean values for each class. Parameters m=2 and r=(0.2* data standard deviation) are used for the SampEn calculation*

time series of healthy young subjects and subjects with CHF are very close, and time series of elderly subjects have the lowest entropy value. However, for the remaining scales, healthy young subjects present the highest entropy values. The entropy values for healthy elderly subjects become a little greater than the CHF subjects for scales from 4 to 7, but not significantly in this case.

3.5 Conclusion

Entropy-based methods appear as a useful tool in the study of cardiac signals, and its possible application as a clinic tool for diagnosis or prediction of different cardiac pathologies is been explored [Schuckers 99, Pincus 01, Lake 02, Magenes 03, Marques-de Sá 05, Costa 05, Ferrario 06].

ApEn is a statistic that characterizes the degree of irregularity of the temporal series. It has been widely applied to the HRV signal study in the last years with promising results. This statistic provides good estimates even with a not too large amount of samples. In principle, *ApEn* is robust to outliers but this fact could be hampered by the choice of the parameter r.

It is not much affected by noise and it can be applied to both, deterministic and stochastic processes, which makes it adequate for the study of biological signals. However, *ApEn* has a bias that makes itself dependent of the data length and it also lacks of relative consistency in many cases.

SampEn statistic is defined in order to minimize these drawbacks. Its algorithm eliminates self-matches when computing probabilities. With this, a reduction of the bias is achieved and therefore the dependence on the data length is reduced as well. *SampEn* also presents relative consistency under circumstances where *ApEn* does not.

While former methods are based on a single scale analysis, the *MSE* method suggests the analysis of the physiological time series in its different temporal scales.

These three methods are not uncorrelated, each one is based on the previous one, but they also have differences that may yield different results when applied. In the following chapter, the performance of these methods will be tested with well known synthetic signals. The influence of parameters m and r in this performance will also be studied in detail.

Chapter 4

Entropy Methods Testing on Synthetic Signals

In this chapter, first a set of synthetic signals of different nature are presented. Afterwards, several experiments are performed over this set of signals in order to test the performance of the entropy methods introduced in the previous chapter. The dependence of *ApEn* and *SampEn* on their free parameters, m and r, and on the data length (N) is tested. Also, the relative consistency of the algorithms is studied. Finally, a *MSE* analysis is performed over some of the synthetic signals.

4.1 Synthetic Signals

In order to asses the behavior of the entropy methods introduced in the previous chapter, some synthetic signals have been chosen, namely, a deterministic signal (sinusoidal signal), a chaotic deterministic signal (logistic map), a signal with both deterministic and stochastic components (MIX process) and a HRV model. Next, a brief description of this set of signals is given.

4.1.1 Sinusoidal Signal

The algorithms are first tested on a deterministic signal, namely a sinusoidal signal, whose expression is given by

$$x = A\sin(2\pi ft + \phi_0) \tag{4.1}$$

where A represents the amplitude, f is the frequency in Hertz, t represents the temporal evolution and ϕ_0 is the initial phase.

4.1.2 Logistic Map

The entropy methods are also tested on a low dimensional non-linear deterministic system known as logistic map (also called quadratic map) [Kaplan 95]. The expression of the logistic map is given by

$$x_{n+1} = Rx_n(1 - x_n) \tag{4.2}$$

According to the election of the R parameter, the following behaviors can be observed:

- Steady state ($0 < R < 3$); the nonlinear equation can have a solution that approaches a certain state and remains fixed there.
- Periodic cycles ($3 < R < 3.5$); the solution to the nonlinear equation can have cycles and oscillate between different values.
- Chaotic dynamics ($3.5 < R < 4$); the solution to the non-linear equation may oscillate, not in a periodic manner, but with chaotic behavior.

For the experiments in this work, $R = 3.8$ is chosen, which corresponds to the last kind of behaviors. In this way, a deterministic chaotic signal is obtained.

4.1.3 MIX Processes

MIX processes are a sort of stochastic signals superimposed on deterministic components, an example of which is as follows:

- First, the value of a certain variable p is fixed to $0 \leq p \leq 1$.
- Second, the sequence $X_n = \sqrt{2}\sin(2\pi n/12)$ -the deterministic component- is defined $\forall n$ where n is the length of the resulting signal.

- Third, Y_n is defined as a family of independent identically distributed (i.i.d.) real random variables, with uniform density on the interval $\left[-\sqrt{3}, \sqrt{3}\right]$.

- Next, Z_n is defined as a family of i.i.d random variables as follows:

  $Z_n = 1$ with probability p.
  $Z_n = 0$ with probability $1 - p$.

- Finally, the $MIX_n = (1 - Z_n)X_n + Z_nY_n$ process is obtained
  where MIX_n represents each sample of the resulting MIX process.

$MIX(p)$ is generated first ascertaining, for each n, whether the nth sample will be obtained from the deterministic sine wave or from the random uniform variable, with likelihood $(1 - p)$ and p respectively, and then calculating X_n or Y_n. Increasing p means therefore greater system randomness [Pincus 91].

4.1.4 Auto-Regressive Models of HRV Signal

In order to test the entropy methods on a more realistic signal, sequences of cardiac beats with the typical spectrum of a healthy subject are generated. For this purpose, two Auto-Regressive (AR) models are used, the first corresponding with a typical PSD distribution in a rest situation, and the second corresponding with a typical PSD distribution in a head-up tilt.

The head-up tilt test is a clinical test used to evaluate patients who have had syncope. The patient is strapped to a table, which is then mechanically tilted to an upright position. During the test, the pulse, blood pressure, electrocardiogram, and blood oxygen saturation can be monitored. When the patient's syncope is reproduced during the test, the test is said to be positive. But the AR models used in this work simulate sequences of cardiac beats of a healthy subject, and in a normal person, blood pressure will not drop dramatically during the test, because the body will compensate for this posture with an increase in heart rate and constriction of the blood vessels in the legs [Fogoros 03].

These PSD distributions in rest situation and in head up tilt are described in [Malik 96] and are considered typical distributions of the PSD of the HRV (Fig.4.1). In this work, the model with the coefficients described in [Mateo 00] is used.

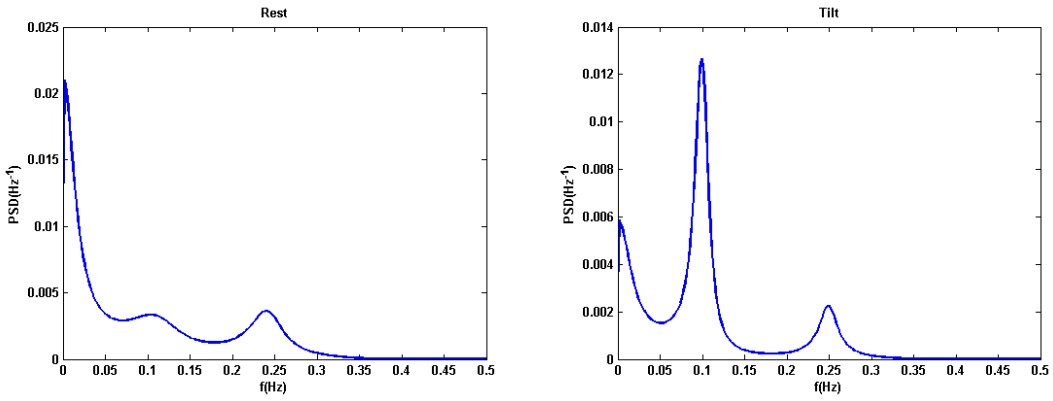

(a) (b)

Figure 4.1: *PSD distributions of HRV signals obtained with the AR models in rest (a) and tilt (b).*

4.2 Tests

Following, different experiments with the presented signals are performed. In these experiments, a comparison between *ApEn* and *SampEn* algorithms is carried out. The dependence on their free parameters m and r, and on the data length N is tested. Also, the relative consistency of both algorithms is compared. Finally, the multiscale approach and the single scale methods are compared.

4.2.1 Entropy Methods Dependence on the Data Length

To test the dependence of the entropy indices against the data length, m and r parameters are set to the most widely used values in the literature [Pincus 91, Richman 00], $m = 2$ and $r = 0.2 * sd$, where sd is the data standard deviation. Then, for different values of the data length, $N = 100, 500, 1000, 2000, 4000, 6000, 8000, 10000, 20000, 40000, 100000$, *ApEn* and *SampEn* are computed. Typically the N values used to compute these indices oscillate between 100 and 5000 samples, but, since in the next chapter, real signals obtained from holter recordings (approximately 100000 samples) will be studied, the synthetic signals in this chapter are also analyzed up to 100000 samples.

In the following set of experiments, in order to distinguish adequately the different degrees of irregularity of the chosen signals, normalized values of the entropies will be shown. The normalization process is the same as that explained in the example 3.2.1.

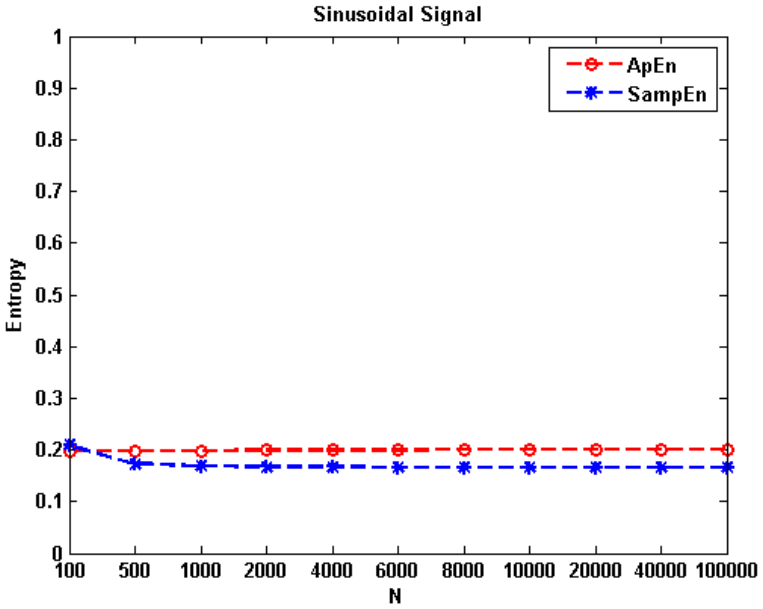

Figure 4.2: *Sinusoidal Signal. ApEn and SampEn dependence on the data length (N). Entropy values have been normalized. Parameters m and r are set to 2 and 0.2*sd respectively.*

Sinusoidal Signal

First, the sinusoidal signal is used to compute *ApEn* and *SampEn* for the different values of the data length.

Figure 4.2, shows *ApEn* and *SampEn* values as a function of data lenght. *ApEn* is approximately independent of data length. *SampEn* is also approximately independent but for N values higher than 100, this could be due to that 100 samples may be not enough to achieve reasonable estimates. For $N = 100$, the *SampEn* value is slightly higher than the *ApEn* value, whereas for the rest values, *ApEn* is a little higher than *SampEn*.

Logistic Map

To continue with the study of the data length dependence, *ApEn* and *SampEn* are evaluated on the logistic map in a deterministic chaotic behavior.

Figure 4.3 shows that *ApEn* is a little lower than *SampEn* for the lowest N value, while both statistics have almost identical results for the remaining N values. In general, *ApEn* and *SampEn* show high independence of the data length. Notice that, since the logistic map is more irregular than the sinusoidal signal, the entropy values are a slightly higher for the logistic map.

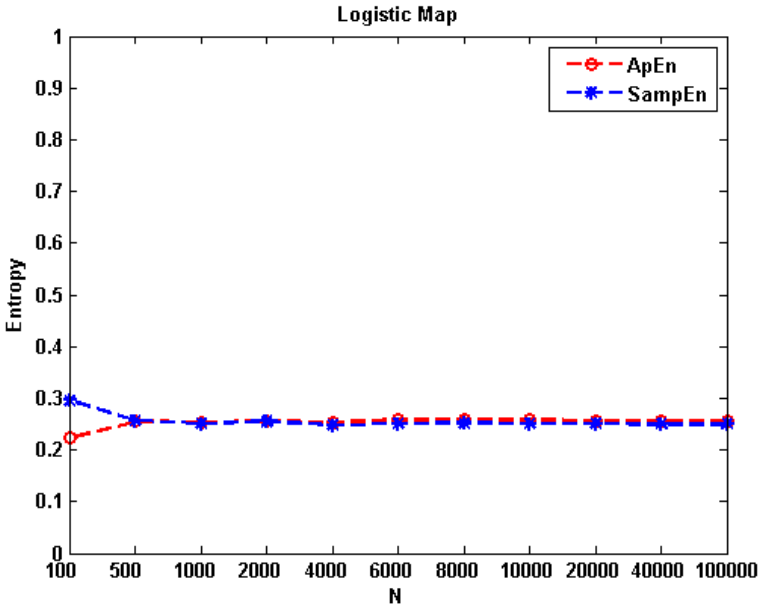

Figure 4.3: *Logistic Map. ApEn and SampEn dependence on the data length (N). Entropy values have been normalized. Parameters m and r are set to 2 and 0.2*sd respectively.*

MIX Processes

To carry on the next test, process MIX(0.5) is chosen, therefore, parameter p is set to $p = 0.5$. Ten realizations of this process are obtained for each value of N; then, the mean and the standard deviation of the results are presented as a function of N (Fig. 4.4).

Entropy values obtained for the MIX process are higher than those obtained for the previous signals. The reason is that it is an stochastic process, and therefore is expected to have a more irregular behavior. *SampEn* results are quite more independent of the data length than the *ApEn* ones. However, it presents hight standard deviation for low values of N; the reason is that *SampEn* does not count self matches, and for an irregular process like the MIX(0.5), it needs a reasonable amount of samples to ensure that the conditional probabilities in its algorithm are reasonably estimated.

ApEn takes longer to stabilize and shows very low values for small data lengths. It achieves a reasonable stabilization from $N = 4000$ samples onwards. For N less than 1000 samples, *ApEn* values are lower than *SampEn* values, while the opposite happens for $N > 1000$, in fact from $N = 4000$ onwards, *ApEn* values are almost uniformly higher than *SampEn* values.

Therefore, for this stochastic signal, *SampEn* is less dependent on the data length than *ApEn*,

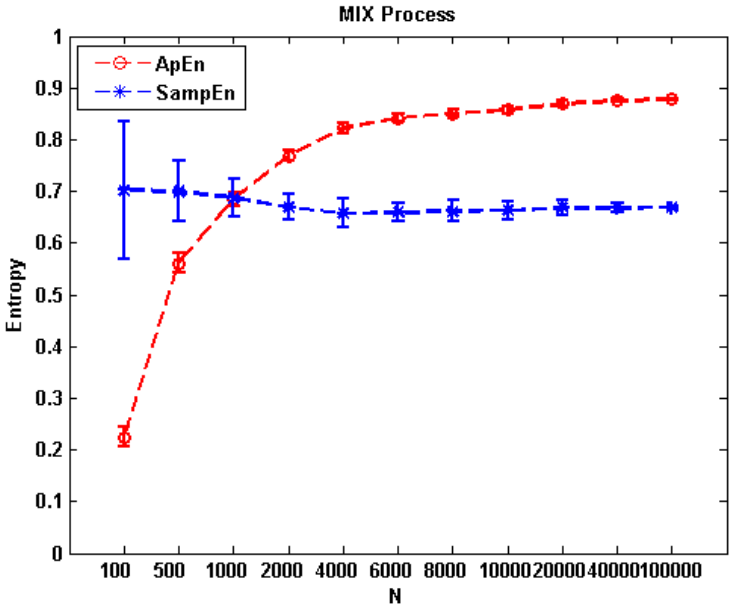

Figure 4.4: *MIX(0.5) process. ApEn and SampEn dependence on the data length (N). Entropy values have been normalized. Parameters m and r are set to 2 and 0.2*sd respectively.*

which agrees with the reported results in [Richman 00], although it presents higher standard deviation for any data length. The *ApEn* results are also almost independent of the data length for high N.

Following, in order to test the algorithms over signals with different degree of irregularity, 4 different values for parameter p are chosen (p=0.1,0.3,0.6,0.9). Ten realizations of each MIX process are obtained, and then *ApEn* and *SampEn* are computed for each process. Once seen that for high number of samples the results are highly independent on data length and due to the high computational cost, for this experiment the highest N value is reduced to 40000 samples.

Figure 4.5 shows the mean and the standard deviation of the results for each MIX process and for each N.

It can be see that both statistics are able to separate these processes with different degree of irregularity, but it is the *SampEn* which achieves the best separation between the processes. Also notice that for very irregular processes and low N values *SampEn* exhibits higher results than *ApEn*, whereas the opposite occurs for more regular processes or for high N values. As already was seen for the MIX(0.5) process, *SampEn* is less dependent on the data length, although it has higher standard deviation for low number of samples.

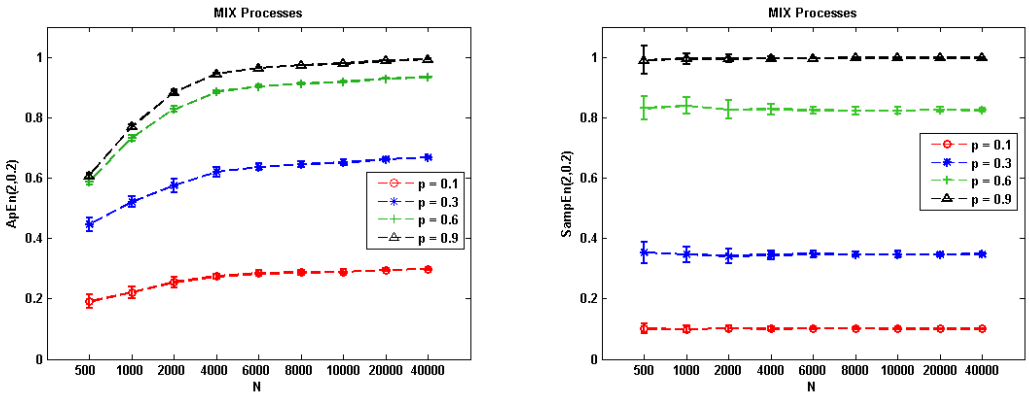

(a) (b)

Figure 4.5: *MIX processes. ApEn and SampEn dependence on the data length (N). Entropy values have been normalized. Parameters m and r are set to 2 and 0.2*sd respectively.*

AR Models

Following, the two AR models corresponding with a typical PSD distribution in a rest situation, and in a head-up tilt, are used to generate synthetic HRV signals that simulate this situations. Ten realizations of each model are obtained and the mean and standard deviation of *ApEn* and *SampEn* are computed as a function of data length.

Figure 4.6 shows that *SampEn* values have first a decreasing tendency which tends to stabilize for very high N values. *ApEn* has the opposite tendency for low number of samples, and also tends to stabilize for very high N values. Notice that *SampEn* has higher standard deviation, mainly for low values of N.

Also notice that for both entropy measures, results in rest situation are higher than in head-up tilt situation, when the symptoms of a syncope are reproduced in a controlled clinical environment.

4.2.2 Entropy Methods Dependence on the Threshold value r

In the following experiments, the signal behavior with regard to the parameter r of the entropy algorithms is tested. For each synthetic signal, *ApEn* and *SampEn* are computed for 30 different values of $r * sd$, with $r \in [0.1, 2.1]$. In these tests, parameter m remains set to 2 and parameter N is fixed to $N = 5000$, since for such value both *ApEn* and *SampEn* have proved to reasonably converge in the studied signals.

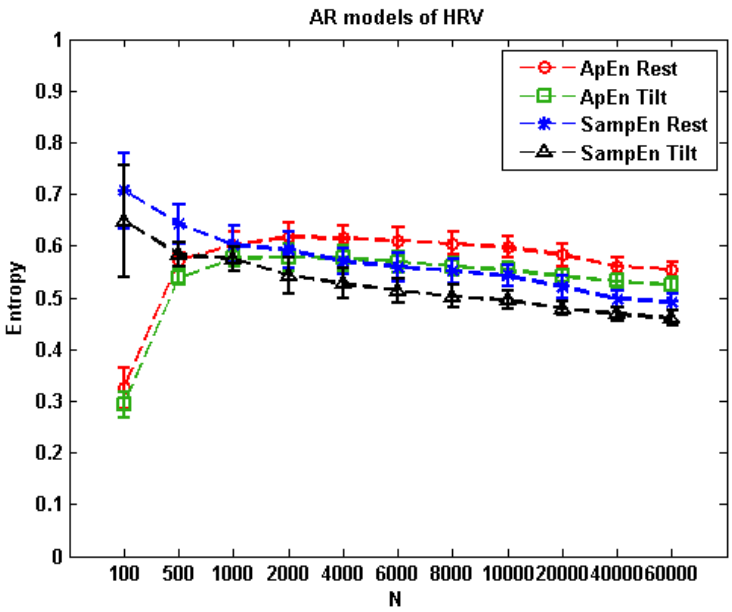

Figure 4.6: *AR models of HRV. ApEn and SampEn dependence on the data length (N). Entropy values have been normalized. Parameters m and r are set to 2 and 0.2*sd respectively.*

For most processes, the conditional probability that sequences similar, with regard to a certain ratio r, remain similar, when the sequences increase in one sample, should decrease as r decreases because the criterion for matching becomes more stringent. Therefore, *ApEn* and *SampEn* are expected to increase as r decreases [Pincus 91, Richman 00].

From now on, in this chapter, normalized entropies are no longer shown, instead, the original values are presented. The reason is that, when we normalize the entropy values by mapping all possible values in the original signal to a limited set of values, 10 values in this case, a coarse grained signal is obtained and a fine study of parameters r and m is no longer possible.

Sinusoidal Signal

For the sinusoidal signal, both *ApEn* and *SampEn*, agree with theory for all the studied r range, i.e. the entropy values decrease as r increases (Fig 4.7).

ApEn exhibits higher values than *SampEn* until $r = 0.2$; beyond this value they both converge toward zero, since the criterion for matching becomes less stringent and almost all the vectors match for m and for $m + 1$ samples.

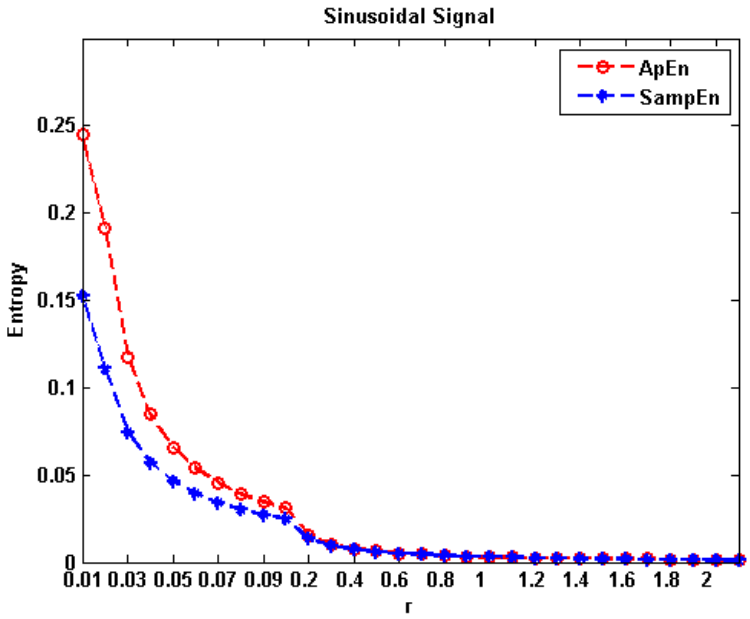

Figure 4.7: *Sinusoidal Signal. Influence of parameter r in the computed ApEn and SampEn values. Parameters m and N are set to 2 and 5000 respectively.*

Logistic Map

For the logistic map, both *ApEn* and *SampEn* agree with theory for all tested values of r, except *ApEn* from the first to the second r values. Both statistics show very similar values for all tested range values. (Fig. 4.8).

In this case, the entropies do not converge toward zero in the tested r range due to two reasons. First, because the logistic map is a more irregular signal than the sinusoidal signal, and second, because its standard deviation (≈ 0.2) is lower than the standard deviation of the sinusoidal signal (≈ 0.7) and we are setting r as a percentage of the standard deviation .

MIX Processes

Ten realizations of the MIX(0.5) process are now obtained for each r value. Next, *ApEn* and *SampEn* are obtained for each r and for each realization. Then, the mean and the standard deviation of the results are shown in Figure 4.9.

ApEn and *SampEn* have increasing values until $r = 0.1$ and $r = 0.2$ respectively; from this points onwards they decrease. For r until 0.04, *ApEn* values are lower than the *SampEn* values, the reason being that for low r there is a very small number of template matches and the *ApEn*

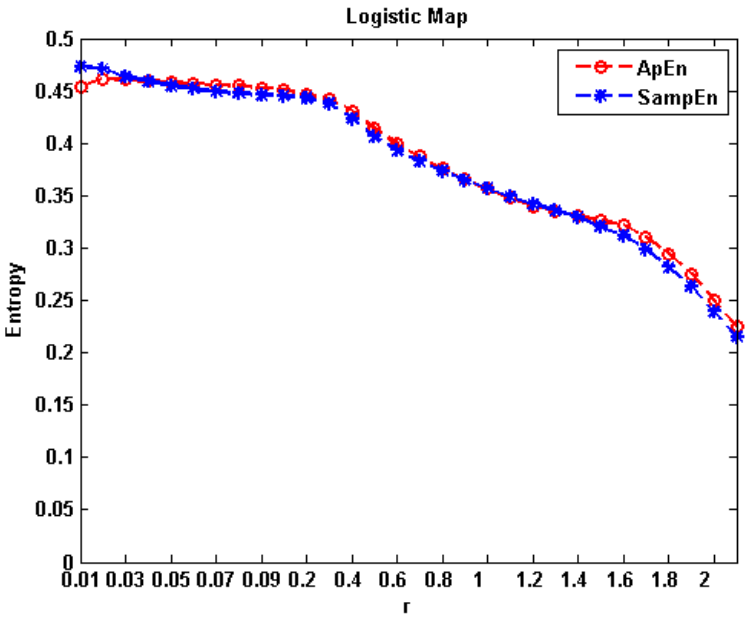

Figure 4.8: *Logistic Map. Influence of parameter r in the computed ApEn and SampEn values. Parameters m and N are set to 2 and 5000 respectively.*

bias is then more marked.

Also notice that for low values of r, the standard deviation of *SampEn* is higher than the standard deviation of *ApEn*. The reason is now the lack of self matches in the *SampEn*. When the matching criterion becomes very strict, the number of vectors similar to other ones are not enough to achieve stable statistics.

AR Models

For AR models, *SampEn* agrees with theory and decreases when r increases, for all tested r values, whereas *ApEn* just fulfills this condition for $r > 0.1$.

For very low r values *ApEn* tends to 0. The reason is that when the filter r is very stringent, there is a very small number of template matches, and the larger deviation of the *ApEn* bias occurs in this situation, when a large proportion of templates do not have matches and are assigned a conditional probability of one, corresponding to perfect order.

As expected, *SampEn* continues to exhibit higher standard deviation for low r values (Fig 4.10).

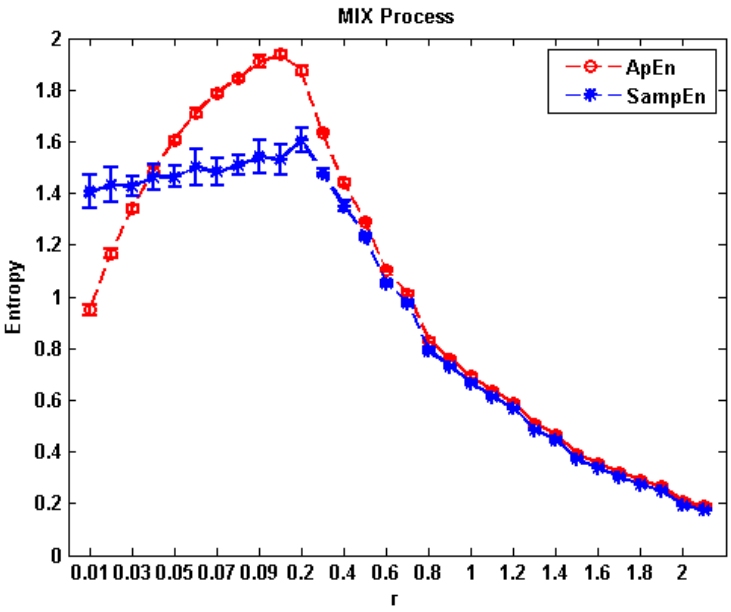

Figure 4.9: *MIX(0.5) process. Influence of parameter r in the computed ApEn and SampEn values. Parameters m and N are set to 2 and 5000 respectively.*

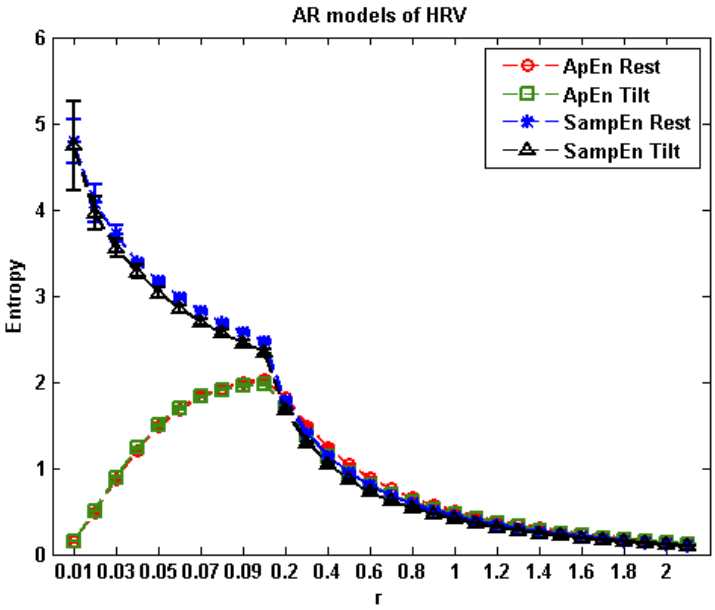

Figure 4.10: *AR models of HRV. Influence of parameter r in the computed ApEn and SampEn values. Parameters m and N are set to 2 and 5000 respectively.*

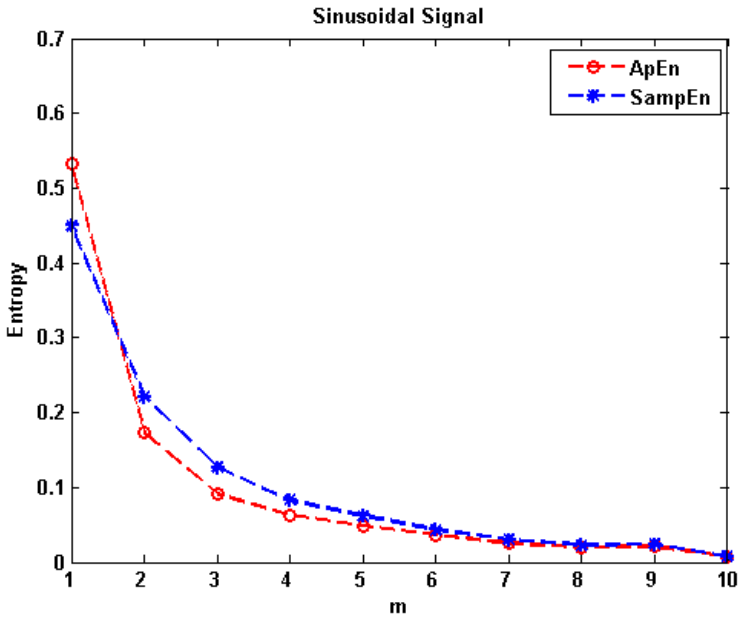

Figure 4.11: *Sinusoidal Signal. Influence of parameter m in the computed ApEn and SampEn values. Parameters r and N are set to 0.2*sd and 5000 respectively.*

4.2.3 Entropy Methods Dependence on the Parameter m

In this section the behavior of the algorithms against the variation of the parameter m is tested. To this purpose, 10 values of m have been chosen, $m = 1, 2, 3, 4, 5, 6, 7, 8, 9, 10$.

In this case, *ApEn* and *SampEn* are expected to decrease as m increases, because the higher the length of the vectors to be compared the lower the probability of them to be similar becomes.

Sinusoidal Signal

Figure 4.11 shows that both *ApEn* and *SampEn* values decrease as m increases. They both follow similar patterns but for $m = 1$ *ApEn* is higher than *SampEn*, while the opposite occurs for remaining m values until $m = 6$; beyond that they both have almost identical results.

Logistic Map

For the logistic Map (Fig. 4.12), *ApEn* and *SampEn* values also decrease as m increases, but in this case, for $m = 1$ *SampEn* is higher than *ApEn*, whereas *ApEn* shows higher values than *SampEn* for the remaining m values.

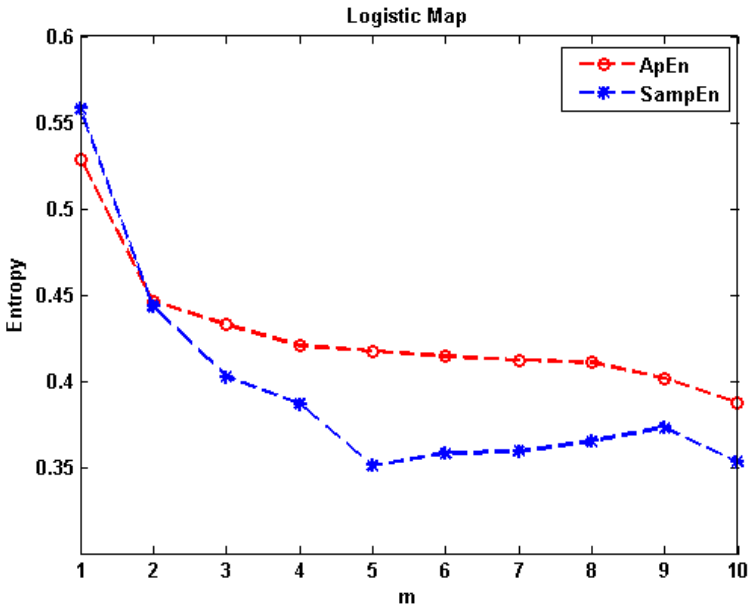

Figure 4.12: *Logistic Map. Influence of parameter m in the computed ApEn and SampEn values. Parameters r and N are set to 0.2*sd and 5000 respectively.*

MIX Processes

Following, 10 realizations of MIX(0.5) process are obtained, for each value of parameter m. *ApEn* and *SampEn* are computed for each m value and for each realization. Figure 4.13 shows the mean and standard deviation of the results.

For low values of m, *ApEn* statistics are higher than the *SampEn* ones (until $m = 3$), then *ApEn* decreases rapidly, while *SampEn* values first decrease slowly and then, they converge to a fixed value.

It is remarkable that the higher the m value, the higher the standard deviation of *SampEn* results becomes. Moreover, *SampEn* is not defined for $m = 10$, which means that there are not even two vectors of 10 samples similar to each other that remain similar for 11 samples, in this signal. Also, for high values of m *ApEn* becomes 0. For this reason, in practice low values of m must be used in order to obtain reasonable statistics.

AR Models

For AR models (Fig 4.14), *ApEn* exhibits higher values for the rest situations until $m = 3$, and then both rest and tilt exhibit very similar values. *SampEn* exhibits higher values for the

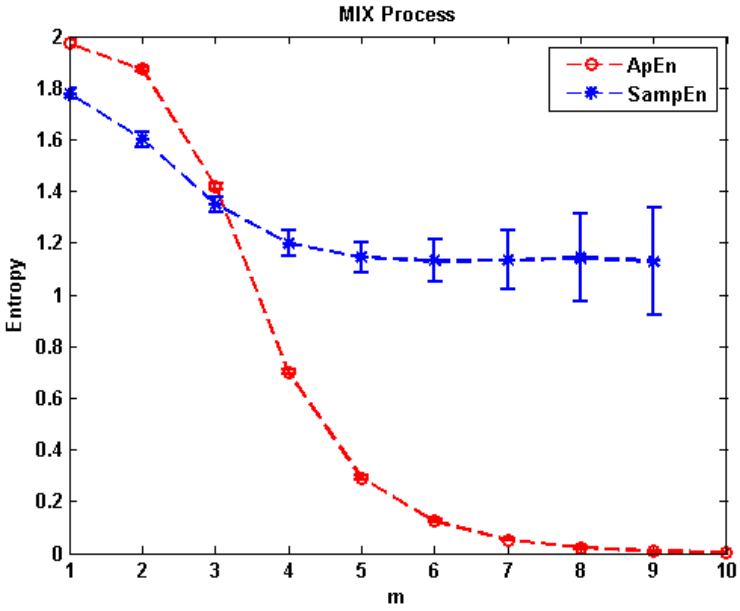

Figure 4.13: *Mix Process. Influence of parameter m in the computed ApEn and SampEn values. Parameters r and N are set to 0.2*sd and 5000 respectively.*

rest situation than for the tilt situation for all m values where is defined, except for $m = 3$, where rest and tilt have the same value.

Notice, that the standard deviation of the *SampEn* increases when m is increased. For both rest and tilt, *SampEn* is defined until $m = 8$, because the probability of not finding similar vectors when m increases, is higher, and therefore also the probability of *SampEn* not being defined.

4.2.4 Relative Consistency

In this section, the relative consistency of *ApEn* and *SampEn* statistics with regard to the variation of their free parameters, r and m, is tested. For this purpose MIX processes with different degrees of irregularity are obtained. Four values of parameter p are chosen ($p = 0.1, 0.3, 0.6, 0.9$) for the MIX processes, and then 10 realizations of each process are obtained, each one with 5000 samples.

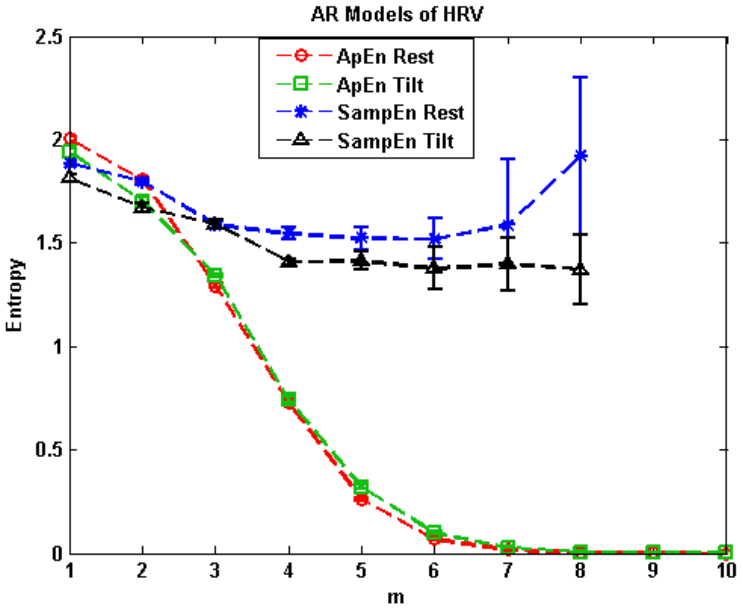

Figure 4.14: *AR models of HRV. Influence of parameter m in the computed ApEn and SampEn values. Parameters r and N are set to 0.2*sd and 5000 respectively.*

Parameter m

First, the relative consistency of the statistics with regard to parameter the m is tested for $m = 1, 2, 3, 4, 5, 6, 7, 8, 9, 10$.

Figure 4.15 shows the mean and the standard deviation of *ApEn* 4.15 (a) and *SampEn* 4.15 (b), for each process and each m value.

ApEn only shows relative consistency for $m = 1$ and $m = 2$, whereas *SampEn* shows relative consistency for all tested values in which it is defined.

Notice that for MIX(0.6), *SampEn* is defined up to $m = 7$, and for MIX(0.9), just until $m = 5$, also, it has high values of standard deviation from $m = 4$ onwards for both processes. The reason is that for very irregular processes is difficult or even impossible to find similar vectors when the length of the vectors (m) increases.

The m values that achieve higher separation between these four processes are, $m = 2$ for *ApEn*, and $m = 3$ for *SampEn*. For the latter, besides the separation between the means, also the standard deviation is considered.

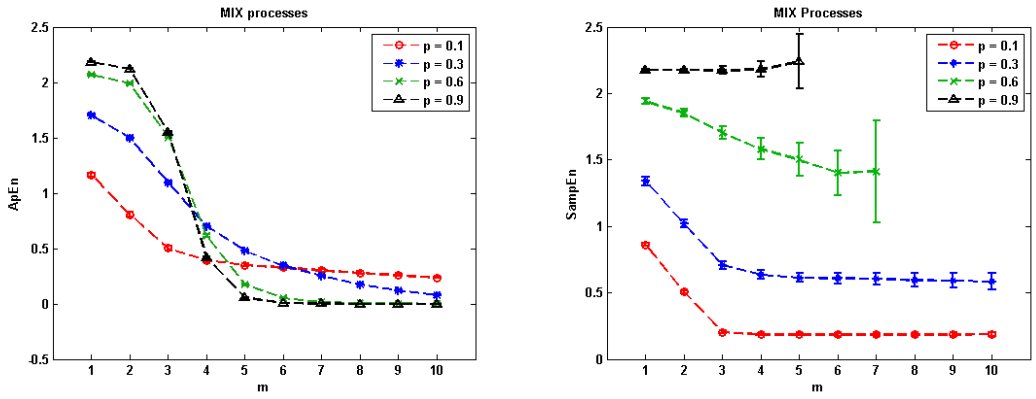

(a) (b)

Figure 4.15: *Testing the relative consistency of the statistics with MIX processes. Variation of parameter m in the compute of ApEn (a) and SampEn (b).*

Parameter r

Following, the relative consistency of the statistics with regard to parameter r is tested. The m parameters are set to $m = 2$ for *ApEn* and to $m = 3$ for *SampEn*, i.e. the values chosen in the previous test.

Figure 4.16 shows the mean of standard deviation of the results. It can be seen that *ApEn* lacks of relative consistency when the whole range of parameter r is observed, but it keeps this relative consistency over the statistically valid range ($r \in [0.1 * sd, 0.25 * sd]$), which is the one used in practice [Pincus 94].

SampEn shows relative consistency until $r = 0.5$, because for high r values, as happens for *ApEn*, the four processes converge toward zero. However, it clearly maintains relative consistency in a larger range than *ApEn* does, and also with a better separation between the four processes.

Notice, that for both indices, the more irregular the process is, the more abruptly the entropy value decreases toward zero for high r values. The reason seems to be that for low r values, the more irregular processes are the ones that still do not have many matched templates, as r increases the number of matched templates is expected to increase more rapidly than the ones in more regular processes.

SampEn is not defined for MIX(0.9) process when r values are very low. In this case, we have a very irregular process and a very restrictive filter. The consequence is that, there are not even two vectors that differ less than 0.04 for both $m = 3$ and $m = 4$, in the whole signal and

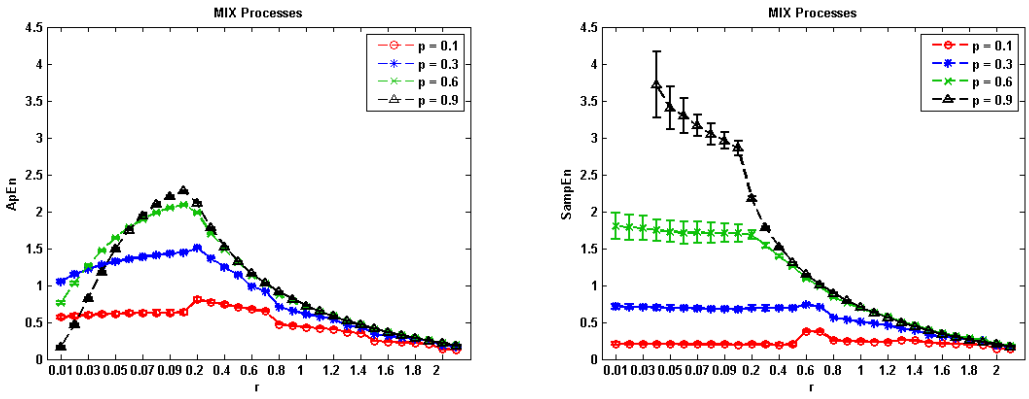

(a) (b)

Figure 4.16: *Testing the relative consistency of the statistics with MIX processes. Variation of parameter r in the compute of ApEn (a) and SampEn (b).*

therefore *SampEn* is not defined for $r < 0.04$.

The r value that better differentiates between the four signals for both *ApEn* and *SampEn* is $r = 0.1$

4.2.5 A Single Scale Methods vs Multiscale Approach

For the following experiment, m and r values that better separated the MIX processes in the previous experiments are used, therefore, *ApEn(2,0.1)* and *SampEn(3,0.1)* are computed. In this experiment a multiscale analysis with 20 scales is performed. The analysis is performed using the MIX processes ($p = 0.1, 0.3, 0.6, 0.9$).

Figure 4.17 shows the results of *ApEn* 4.17 (a) and *SampEn* 4.17 (b), for each process and for each scale factor. These results agree with the ones in [Ferrario 06], and as can be seen, the maximum separation for the processes occurs for the first scale factor, that is, for the original signal. Therefore, the multiscale approach does not reveal further relevant information about the MIX processes, related to the separation of processes with different degree of irregularity, than the single scale methods.

Following, the same analysis is performed on the AR models of HRV. Figure 4.18 shows that both statistics follow the same patterns, for the original signal, $\tau = 1$, the rest models show higher entropy values. Then, for $\tau = 2$, rest and tilt situations present the same values. For a few following scale factors, tilt model shows higher results and finally, again the rest model

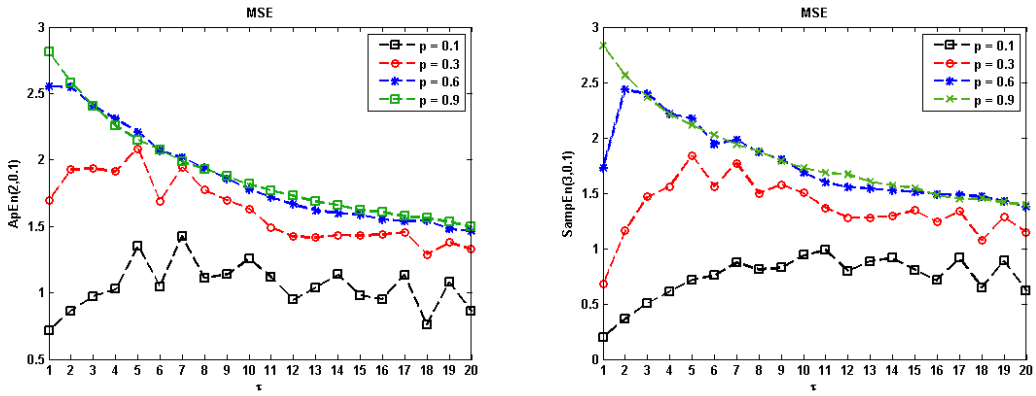

(a) (b)

Figure 4.17: *Results of the MSE analysis with 20 scales for MIX processes, with ApEn (a) and SampEn (b).*

presents higher results. Therefore, for the AR models of HRV is also not possible to extract any further information by the multiscale analysis.

Since with the chosen synthetic signals the usefulness of the multiscale approach cannot be appreciated, in the next chapter the *MSE* method will be computed over real signals in order to test its performance.

4.3 Conclusion

In this chapter properties and performance of the entropy methods introduced in the previous chapter have been tested on synthetic signals. The conclusions of these tests can be divided in two parts, on one hand, the conclusions about the behavior of the algorithms itself and on the other hand the conclusions about the comparison between the two statistics and the selection of the free parameters.

First, from the behavior of the algorithms several points are worth noticing:

- Due to the fact that *ApEn* counts self template matches, it has a bias that makes itself dependent on the data length and uniformly lower than expected, as explained in [Pincus 94, Richman 00]. This characteristics have been corroborated in this work for very irregular signals and in general for a not very large amount of samples, until $N < 5000$ approximately. However, more regular signals like, MIX(0.1) or MIX(0.3), show higher *ApEn*

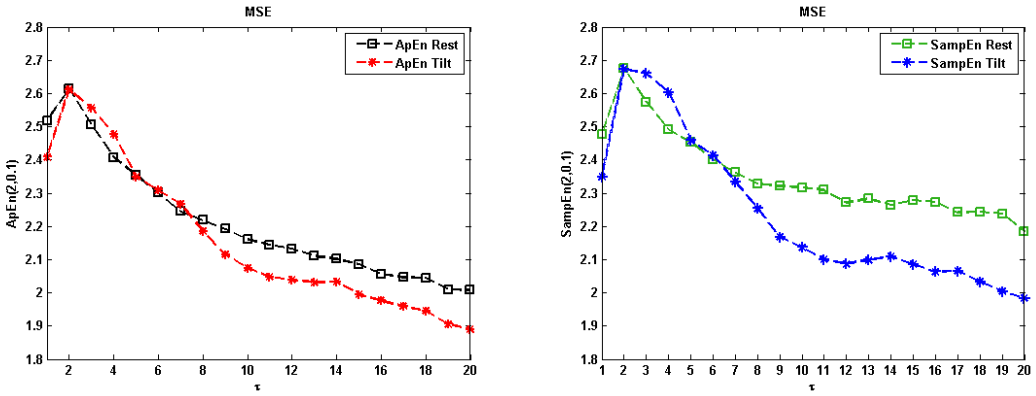

(a) (b)

Figure 4.18: *Results of the MSE analysis with 20 scales for AR models of HRV, with ApEn (a) and SampEn (b).*

than *SampEn* for all tested data lengths and also the MIX(0.5), MIX(0.6) and the AR models of HRV, for high N values. This fact can also be appreciate in [Richman 00] where *ApEn* and *SampEn* are computed over MIX(0.1) and MIX(0.9) processes.

- Regarding the performance of the algorithms against parameter r, *SampEn* agrees with theory in more situations than *ApEn* does. The reason is that for very low r values there is a very small number of template matches and the bias of the *ApEn* is more marked in that situation.

- In tests for parameter m, for hight m values and irregular signals, namely, MIX(0.5) and AR models, *ApEn* tends toward zero whereas *SampEn* does not, because the small number of template matches makes the *ApEn* bias more marked. Likewise, due to the lack of template matches, for high m values *SampEn* is not defined or has high standard deviation.

  For more regular signals, sinusoidal and logistic map, they both decrease as m increases as expected.

- *SampEn* shows relative consistency in more situations than *ApEn* does.

- The *MSE* analysis performed over the MIX processes and AR models did not reveal further relevant information, related to the separation of processes with different degree of irregularity, than the single scale methods.

Second, about the comparison between the two statistics and the selection of the free parameters:

- From the experiments performed in this chapter, can be concluded that although *SampEn* is sometimes not defined for extreme values of its free parameters, in the statistical valid range of these parameters, it achieves a better separation of processes of well known irregularity than *ApEn*. Furthermore, *SampEn* agrees with theory in more situations, than *ApEn* does. For this reason and also due to the high computational cost of the tests, experiments with real data will only be performed with the *SampEn* statistic.

- The parameters that achieved best separation for the different MIX processes cannot be taken as the more suitable for real data but, from the performed tests, the statistically valid range of the parameters has been corroborated. Therefore, in the experiments with real data, the test ranges will be reduced to $m = [1, 2, 3]$ and $r = [0.1, 0.15, 0.2]$.

Chapter 5

Entropy Methods Testing on Real Signals

In this chapter, tests are performed on real signals from healthy subjects and from subjects with Congestive Heart Failure (CHF). The main objectives are two: First, use *SampEn* statistic to discriminate between healthy and pathological subjects, and second, asses the loss of HRV due to aging in healthy subjects by using *SampEn*.

With these goals, first, the influence of the free parameters tuning in the performance of the statistic is studied, with the aim of maximizing the separation between healthy and pathological subjects.

Next, the discrimination capabilities of the statistics to distinguish between young and elderly groups of healthy subjects are also studied. Finally, the recordings are split into different groups according to the age of the subjects, and the evolution of the statistic is analyzed.

In the end, a *MSE* analysis is performed with the real data.

5.1 Datasets

Entropy methods are used to asses the variability of the RR-interval signals derived from 24-hour Holter recordings from healthy subjects and from subjects with CHF. Both sets of recordings were obtained from the Physionet database [Goldberger 3].

The data of the healthy group were obtained from 24-hour Holter monitor recordings of 72 healthy subjects, 35 men and 37 women aged from 20 to 76 years old. The data of the CHF group were obtained from 24-hour Holter monitor recordings of 44 subjects, from 22 to 79 years old, including 19 men and 6 women (the gender information was not available for all the

recordings).

Some of the recordings from both groups have time information, which is used in this work to study the variation of HRV during different periods of the day (18 healthy subjects aged from 20 to 50 years old, and 15 subjects with CHF aged from 22 to 71 years old).

All data sets were filtered to remove artifacts, missed detections and isolated ectopic beats. Furthermore, RR intervals lower than 200 ms and greater than 2000 ms were removed as well as those which differed more than 20% from the previous and the subsequent RR intervals [Malik 89].

5.2 Introduction

The study is divided in two main parts, on one hand, the discrimination between healthy and pathological subjects using *SampEn* is pursued, and on the other hand, the relation of *SampEn* with aging is studied. For both parts, the influence of the free parameters is tested. For this purpose, a set of possible values for $m = 1, 2, 3$ is evaluated. Concerning to threshold value r, *SampEn* is computed according to two methods:

1. Method 1: parameter r set to a certain percentage of the standard deviation (sd) of each data series, which is the method conventionally used in the literature [Pincus 94, Richman 00, Costa 03b, Signorini 98] (using $r = 0.1, 0.15, 0.2 * sd$).

2. Method 2: parameter r set to a percentage of the mean standard deviation of whole recordings (from healthy and CHF subjects), which means a fixed r for all the recordings (using $r = 10, 15, 20$).

This last method is justified in [Marques-de Sá 05], where better results were reported in Fetal Heart Rate (FHR) Variability assessment by setting r fixed for all the datasets.

5.3 Discriminating Tests for Healthy and CHF Subjects

Discriminating tests for healthy and pathological subjects are divided in two parts:

- First, only the recordings with available time information are used, in order to obtain *SampEn* values for the night period (24:00 - 06:00), the day period (8:00 - 24:00) and the whole recording time (approx. 24 hour).

- Second, all the recordings are taken into account, and *SampEn* is computed for all of them in the entire recording time.

5.3.1 Tests for Different Time Periods

The tests in this section are divided according to the method of setting parameter r. First, the tests using method 1 are performed, and then the tests using method 2.

Since the number of recordings with time information is not large enough (< 25) to assume a normal distribution of the data average values, the Lilliefors test allowed to accept the normality hypothesis at the 1% significance level at least, for all the experiments.

Tests with Variable Threshold Value r

First, parameter r is set by method 1. Table 5.1 shows the results for the different possible combinations of r and m values, for both, healthy and pathological groups, and for each time period.

Major differences between the means are obtained for the night period. For this period some of the combinations of m and r give significant differences in the Student's t test for the means ($p < 0.05$) (See Table 5.1). For the day period and for the 24 hour period, significant differences are not found for any combination of m and r.

For the day period, CHF group has higher mean *SampEn* values than the healthy group, for most of the parameter combinations. Whereas for the night period healthy subjects have higher values of *SampEn* than the pathological subjects. This is due to the fact that *SampEn* increases in the night period with respect to the day period, and although this increase is present for both, healthy an pathological groups, is by far more marked for the healthy group.

For the 24 hour period, healthy subjects obtain higher values than the CHF ones in most of the cases, but with very small differences between the means.

Figure 5.1 (a), (c) and (e) shows the parameters combinations that show larger discrimination (lower p-value in the t test), for each period. Note that these parameter combinations are the same for the day period, and the 24 hour periods, $m = 2$ and $r = 0.15sd$, and different for the night period, $m = 1$ and $r = 0.1sd$.

Table 5.1: *Mean ± sd of SampEn for r set by method 1. Significant variation ($p < 0.05$) between pathological and healthy subjects has been highlighted.*

	CHF			Healthy		
$SampEn(m, r)$	Nigth	Day	24 hour	Nigth	Day	24 hour
$SampEn(3, 0.1sd)$	$\mathbf{1.39 \pm 0.41}$	1.23 ± 0.44	1.10 ± 0.45	$\mathbf{1.76 \pm 0.50}$	1.20 ± 0.25	1.09 ± 0.23
$SampEn(2, 0.1sd)$	$\mathbf{1.47 \pm 0.41}$	1.31 ± 0.45	1.18 ± 0.44	$\mathbf{1.98 \pm 0.53}$	1.30 ± 0.26	1.20 ± 0.26
$SampEn(1, 0.1sd)$	$\mathbf{1.59 \pm 0.40}$	1.45 ± 0.46	1.32 ± 0.45	$\mathbf{2.12 \pm 0.53}$	1.43 ± 0.29	1.34 ± 0.26
$SampEn(3, 0.15sd)$	1.21 ± 0.45	0.92 ± 0.38	0.77 ± 0.42	1.22 ± 0.27	0.97 ± 0.18	0.86 ± 0.26
$SampEn(2, 0.15sd)$	1.29 ± 0.43	1.00 ± 0.38	0.84 ± 0.42	1.42 ± 0.28	1.06 ± 0.20	0.96 ± 0.27
$SampEn(1, 0.15sd)$	1.40 ± 0.43	1.13 ± 0.41	0.98 ± 0.44	1.54 ± 0.29	1.17 ± 0.20	1.07 ± 0.27
$SampEn(3, 0.2sd)$	$\mathbf{0.80 \pm 0.38}$	0.68 ± 0.32	0.59 ± 0.35	$\mathbf{1.05 \pm 0.29}$	0.70 ± 0.15	0.63 ± 0.18
$SampEn(2, 0.2sd)$	$\mathbf{0.86 \pm 0.40}$	0.74 ± 0.32	0.65 ± 0.34	$\mathbf{1.23 \pm 0.34}$	0.77 ± 0.16	0.71 ± 0.20
$SampEn(1, 0.2sd)$	$\mathbf{0.97 \pm 0.36}$	0.87 ± 0.35	0.78 ± 0.36	$\mathbf{1.33 \pm 0.34}$	0.85 ± 0.16	0.80 ± 0.19

Tests with Fixed Threshold Value r

Second, parameter r is set by method 2. Table 5.2 shows the results for the different possible combinations of r and m values, for both, healthy and pathological groups, and for each time period.

For fixed r, a considerably larger discrimination between CHF and healthy subjects is achieved for the three time periods and for any choice of parameters m and r. All the experiments give significant differences ($p < 10^{-4}$) (See Tab 5.2).

SampEn increases for the night period respect to the day period, and for both healthy and pathological groups. This could be due to the fact that during the day period, besides the complex physiological fluctuations that modulate the HR, other fluctuations with more regular patterns, which are the response to changes in the environmental conditions, are present, and this last fluctuations may disguise the irregularity inherent in the HRV signal.

SampEn also presents higher standard deviation for the night time period than for the others.

Larger discrimination between healthy and pathological subjects is obtained for the day and

Table 5.2: *Mean ± sd of SampEn for r set by method 2. Significant variation ($p < 10^{-4}$) between pathological and healthy subjects has been highlighted.*

	CHF			Healthy		
$SampEn(m, r)$	Nigth	Day	24 hour	Nigth	Day	24 hour
$SampEn(3, 10)$	**0.66 ± 0.22**	**0.52 ± 0.16**	**0.53 ± 0.15**	**1.36 ± 0.38**	**1.15 ± 0.23**	**1.16 ± 0.23**
$SampEn(2, 10)$	**0.72 ± 0.25**	**0.58 ± 0.18**	**0.60 ± 0.18**	**1.57 ± 0.44**	**1.25 ± 0.25**	**1.29 ± 0.25**
$SampEn(1, 10)$	**0.82 ± 0.25**	**0.71 ± 0.21**	**0.73 ± 0.21**	**1.70 ± 0.49**	**1.37 ± 0.26**	**1.43 ± 0.27**
$SampEn(3, 15)$	**0.45 ± 0.19**	**0.33 ± 0.13**	**0.35 ± 0.13**	**1.36 ± 0.38**	**1.15 ± 0.23**	**1.16 ± 0.23**
$SampEn(2, 15)$	**0.50 ± 0.21**	**0.39 ± 0.15**	**0.40 ± 0.15**	**1.57 ± 0.44**	**1.25 ± 0.25**	**1.29 ± 0.25**
$SampEn(1, 15)$	**0.59 ± 0.21**	**0.50 ± 0.18**	**0.52 ± 0.17**	**1.70 ± 0.49**	**1.37 ± 0.26**	**1.43 ± 0.27**
$SampEn(3, 20)$	**0.25 ± 0.14**	**0.18 ± 0.09**	**0.18 ± 0.09**	**0.97 ± 0.34**	**0.77 ± 0.19**	**0.79 ± 0.20**
$SampEn(2, 20)$	**0.29 ± 0.15**	**0.15 ± 0.08**	**0.23 ± 0.10**	**1.14 ± 0.40**	**0.85 ± 0.21**	**0.88 ± 0.22**
$SampEn(1, 20)$	**0.36 ± 0.16**	**0.30 ± 0.13**	**0.32 ± 0.13**	**1.25 ± 0.45**	**0.94 ± 0.22**	**0.99 ± 0.23**

24 hour period than for the night period.

It is also remarkable that for fixed r, healthy subjects show higher *SampEn* values for the three time periods, which is in agreement with the idea of loss of HRV in pathological conditions.

Figure 5.1 (b), (d) and (f) shows the parameters combinations that show larger discrimination (lower p-value), for each time period. These parameter combinations are, $m = 3$ and $r = 15$ for the day and 24 hour periods, and $m = 2$, $r = 15$ for the night period.

The reason for obtaining better results by setting a fixed r, instead of setting r as a percentage of each data series standard deviation, could be that subjects with CHF have lower standard deviation than the healthy ones (see Table 5.3), and therefore, the relative differences among samples could not be fairly preserved when each recording is divided by its standard deviation in the computation of the distance between samples.

As an example, Table 5.4 shows two data series, each one with four samples of RR-intervals. The first one from a healthy subject and the second one from a CHF subject. The standard deviation of each data series is also presented. Following, the distance between the two first samples is computed, by setting $m = 1$ and r to a certain percentage of each data series standard deviation,

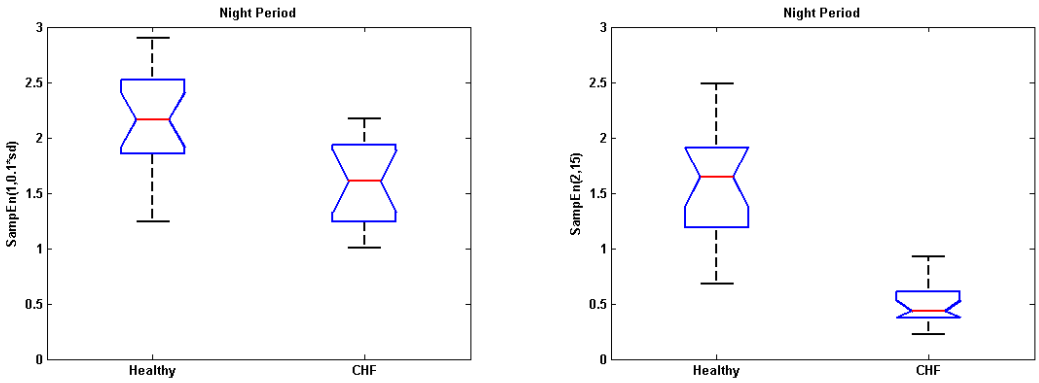

(a)

(b)

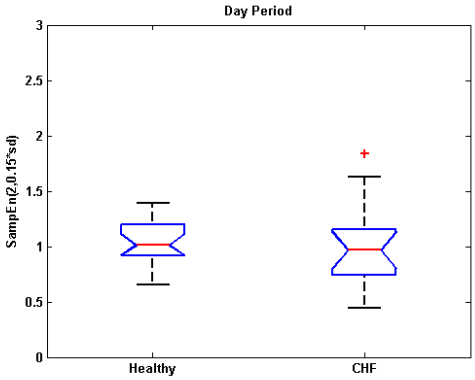

(c)

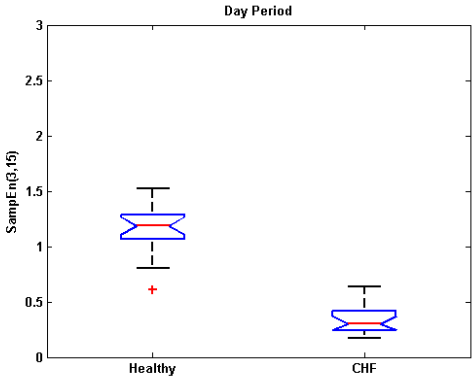

(d)

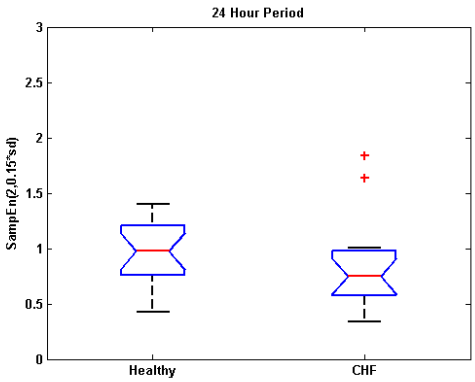

(e)

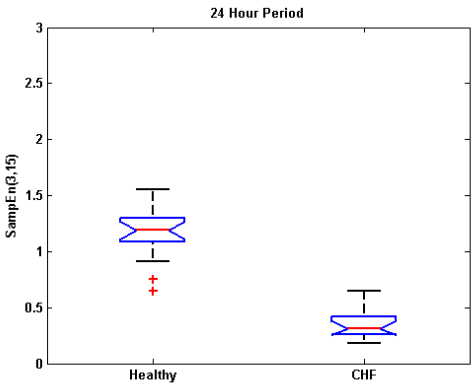

(f)

Figure 5.1: *Boxplot for SampEn computed with r set by method 1 a), c) and e); and with r set by method 2 b), d) and f). For night period a) and b). For day period c) and d). For 24 hour e) and f). The boxes have lines at the lower quartile, median, and upper quartile values. Whiskers extend from each end of the box to 1.5 times the interquartile range. Outliers are displayed with a + sign. Notches display the variability of the median between samples.*

Table 5.3: *Standard deviation of the different groups. Mean ± sd.*

	Standard Deviation
Healthy	136.84±32.67
Healthy-Young	136.20±35.51
Healthy-Elderly	137.20±31.36
CHF	66.98±38.87

Table 5.4: *The table shows four samples of RR-intervals from a healthy subject and from a CHF subject. The standard deviation of each data series is showed.*

	RR_1(ms)	RR_2(ms)	RR_3(ms)	RR_4(ms)	Standard Deviation
Healthy	844	867	891	844	22.46
CHF	580	592	596	592	6.93

- For the healthy subject we have the following situation,

$$\begin{aligned} |844 - 867| &= 23 \leq r \times 22.46 \\ 23/22.46 &\leq r \\ 1.02 &\leq r \end{aligned}$$

- Whereas for the CHF subject we have,

$$\begin{aligned} |580 - 592| &= 12 \leq r \times 6.93 \\ 12/6.93 &\leq r \\ 1.7 &\leq r \end{aligned}$$

For method 2 of setting r, the comparison between the samples would be $23 \leq r$ for the healthy subject and $12 \leq r$ for the CHF subject, while for method 1 of setting r, the comparison would be $1.02 \leq r$ for the healthy subject and $1.7 \leq r$ for the CHF subject. Therefore, with method 1, recordings from healthy subjects are scaled by higher values than recordings from CHF subjects, which does not only affect the amplitude of the data, but also the relative difference between samples.

Table 5.5: *Mean ± sd of SampEn computed by segments over the 24 hour period, for r set by method 2. Significant variation ($p < 10^{-6}$) between pathological and healthy subjects has been highlighted.*

	CHF			Healthy		
$SampEn(m,r)$	Nigth	Day	24 hour	Nigth	Day	24 hour
$SampEn(3,10)$	$\mathbf{0.64 \pm 0.21}$	$\mathbf{0.51 \pm 0.17}$	$\mathbf{0.53 \pm 0.16}$	$\mathbf{1.32 \pm 0.36}$	$\mathbf{1.15 \pm 0.23}$	$\mathbf{1.20 \pm 0.24}$
$SampEn(2,10)$	$\mathbf{0.69 \pm 0.23}$	$\mathbf{0.56 \pm 0.19}$	$\mathbf{0.59 \pm 0.18}$	$\mathbf{1.51 \pm 0.41}$	$\mathbf{1.25 \pm 0.25}$	$\mathbf{1.32 \pm 0.26}$
$SampEn(1,10)$	$\mathbf{0.77 \pm 0.24}$	$\mathbf{0.65 \pm 0.21}$	$\mathbf{0.68 \pm 0.19}$	$\mathbf{1.65 \pm 0.46}$	$\mathbf{1.36 \pm 0.26}$	$\mathbf{1.44 \pm 0.29}$
$SampEn(3,15)$	$\mathbf{0.43 \pm 0.19}$	$\mathbf{0.32 \pm 0.14}$	$\mathbf{0.34 \pm 0.13}$	$\mathbf{1.32 \pm 0.36}$	$\mathbf{1.15 \pm 0.23}$	$\mathbf{1.20 \pm 0.24}$
$SampEn(2,15)$	$\mathbf{0.47 \pm 0.20}$	$\mathbf{0.36 \pm 0.15}$	$\mathbf{0.39 \pm 0.15}$	$\mathbf{1.51 \pm 0.41}$	$\mathbf{1.25 \pm 0.25}$	$\mathbf{1.32 \pm 0.26}$
$SampEn(1,15)$	$\mathbf{0.54 \pm 0.21}$	$\mathbf{0.45 \pm 0.17}$	$\mathbf{0.47 \pm 0.16}$	$\mathbf{1.65 \pm 0.46}$	$\mathbf{1.36 \pm 0.26}$	$\mathbf{1.44 \pm 0.29}$
$SampEn(3,20)$	$\mathbf{0.23 \pm 0.14}$	$\mathbf{0.16 \pm 0.10}$	$\mathbf{0.17 \pm 0.09}$	$\mathbf{0.93 \pm 0.32}$	$\mathbf{0.77 \pm 0.20}$	$\mathbf{0.81 \pm 0.21}$
$SampEn(2,20)$	$\mathbf{0.26 \pm 0.15}$	$\mathbf{0.19 \pm 0.11}$	$\mathbf{0.20 \pm 0.11}$	$\mathbf{1.09 \pm 0.37}$	$\mathbf{0.85 \pm 0.21}$	$\mathbf{0.91 \pm 0.23}$
$SampEn(1,20)$	$\mathbf{0.31 \pm 0.16}$	$\mathbf{0.25 \pm 0.13}$	$\mathbf{0.26 \pm 0.12}$	$\mathbf{1.20 \pm 0.42}$	$\mathbf{0.93 \pm 0.23}$	$\mathbf{1.00 \pm 0.26}$

Computationally Efficient Method of Calculating *SampEn* for 24-hour Holter Recordings

The computation of *SampEn* on large data series has very high computational cost. If a real life application is aimed to be implemented, the computing time should be reduced. For this purpose, in this section a method of calculating the *SampEn* of the data series in an efficient way, in terms of time, is studied.

First, the recordings are divided into non-overlapping segments of 4000 samples (one hour of recording approximately); next, *SampEn* is computed for each segment, and finally the mean of the *SampEn* values is calculated.

For this study, parameter m is set to $1, 2, 3$ and r to $10, 15, 20$ in order to compare the results with the ones obtained on the previous section. Table 5.5 shows the results for the different possible combinations of r and m values, for both, healthy and pathological groups, and for each time period. All the parameter combinations give significant differences ($p < 10^{-6}$).

Figure 5.2 shows the parameter combinations exhibiting larger discrimination for each time period. It also shows the plots obtained in the previous section, where the *SampEn* was computed in a single step for the whole recording length, in order to allow a better visual comparison between the two approaches. Note that the parameter combinations that give larger discrimination are the same for both approaches, $r = 15$ for the three time periods, $m = 2$ for the night period and $m = 3$ for the day and 24 hour periods.

Obtaining *SampEn* by the segments approach severely reduces the computation time, about 20 times less of computation time is needed, which means that a 24 hour recording (approx. 100.000 samples) which needs 80 min of computation time by computing it in a single step for the whole recording length, with the segments approach needs 4 min of computation time[1]. This approach also maintains the discriminating capabilities between healthy and pathological subjects.

5.3.2 Tests For 24 Hour

In this section all the recordings are used to perform the tests, and therefore only the time period of 24 hour is now considered. Free parameters are set to $m = 1, 2, 3$, and r is set using methods 1 and 2. The approach of *SampEn* computation by segments is used.

First, method 1 of setting r is studied. Table 5.6 presents the results for all the possible combinations of m and r, for healthy and CHF groups, and for both methods of setting r. All the experiments give significant differences ($p < 0.05$).

Figure 5.3 (a) shows the box plot of the parameter combination that achieve higher discrimination (lower p-value in the t test).

Second, r is set according to the method 2, Table 5.6 presents the results for all the possible combinations of m and r, for CHF and healthy groups. All the parameter combinations give significant differences ($p < 10^{-13}$).

Figure 5.3 shows the results for both methods of setting r. The parameter combination that achieves greater discrimination for each method is shown. Method 2 of setting r achieves higher discrimination between the CHF and the healthy groups, and also gives higher *SampEn* values for the healthy group than for the pathological group.

Note that since in this section, both healthy and pathological groups have similar age ranges

[1]Computations were made with an Intel Core 2 at 1.67 GHz and 2046 MB of RAM.

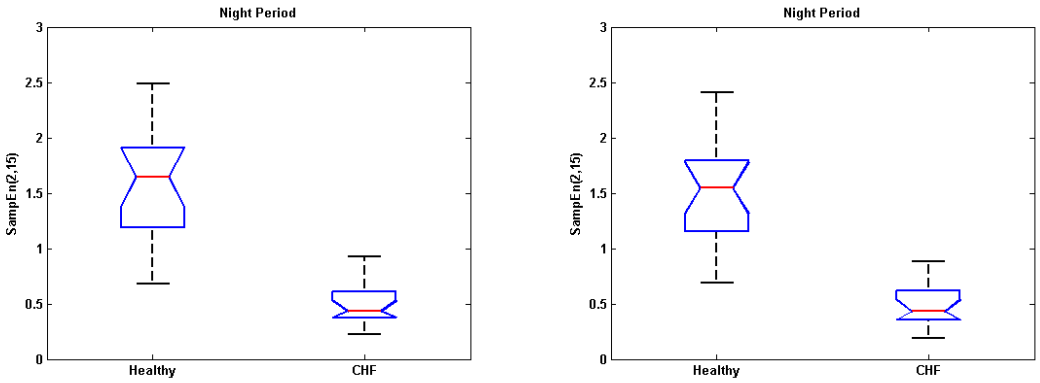

(a)

(b)

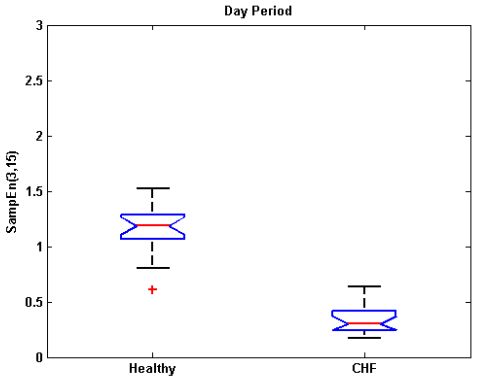

(c)

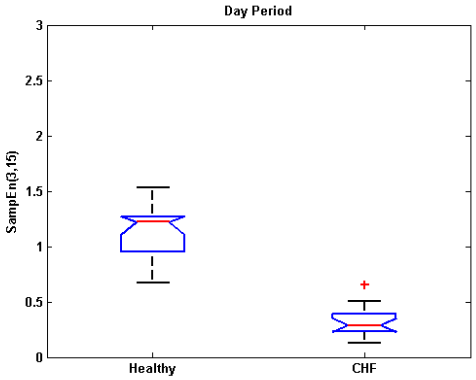

(d)

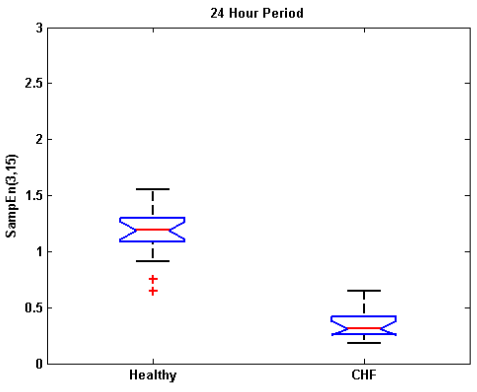

(e)

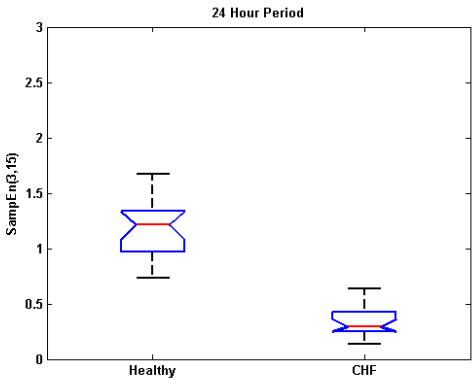

(f)

Figure 5.2: *Boxplot for SampEn computed in a single step for the whole recording length, with r set by method 2 a), c) and e). SampEn computed by segments over the 24 hour period, with r set by method 2 b), d) and f). For night period a) and b) . For day period c) and d). For 24 hour e) and f). The boxes have lines at the lower quartile, median, and upper quartile values. Whiskers extend from each end of the box to 1.5 times the interquartile range. Outliers are displayed with a + sign. Notches display the variability of the median between samples.*

Table 5.6: *Mean ± sd of SampEn computed by segments over the 24 hour, for both methods of setting r. All the available recordings are used. Significant variation between pathological and healthy subjects has been highlighted ($p < 0.05$ for r set by method 1 and $p < 10^{-13}$ for r set by method 2).*

$SampEn(m, rsd)$	CHF	Healthy	$SampEn(m, r)$	CHF	Healthy
$SampEn(3, 0.1sd)$	**1.16 ± 0.36**	**0.91 ± 0.23**	$SampEn(3, 10)$	**0.58 ± 0.23**	**1.00 ± 0.23**
$SampEn(2, 0.1sd)$	**1.24 ± 0.35**	**0.99 ± 0.26**	$SampEn(2, 10)$	**0.64 ± 0.25**	**1.08 ± 0.26**
$SampEn(1, 0.1sd)$	**1.37 ± 0.36**	**1.09 ± 0.27**	$SampEn(1, 10)$	**0.75 ± 0.25**	**1.18 ± 0.27**
$SampEn(3, 0.15sd)$	**0.83 ± 0.39**	**0.66 ± 0.23**	$SampEn(3, 15)$	**0.51 ± 0.25**	**1.00 ± 0.23**
$SampEn(2, 0.15sd)$	**0.90 ± 0.39**	**0.72 ± 0.26**	$SampEn(2, 15)$	**0.57 ± 0.28**	**1.08 ± 0.26**
$SampEn(1, 0.1sd)$	**1.01 ± 0.41**	**0.80 ± 0.27**	$SampEn(1, 15)$	**0.68 ± 0.29**	**1.18 ± 0.27**
$SampEn(3, 0.2sd)$	**0.62 ± 0.33**	**0.47 ± 0.17**	$SampEn(3, 20)$	**0.28 ± 0.18**	**0.64 ± 0.20**
$SampEn(2, 0.2sd)$	**0.68 ± 0.33**	**0.52 ± 0.19**	$SampEn(2, 20)$	**0.32 ± 0.20**	**0.70 ± 0.22**
$SampEn(1, 0.2sd)$	**0.78 ± 0.34**	**0.58 ± 0.20**	$SampEn(1, 20)$	**0.39 ± 0.21**	**0.78 ± 0.24**

(see 5.1), a more balanced study is performed. The increased separation between groups in the previous section, for method 2 of setting r, may be due to the fact that the CHF group had a larger age range than the healthy group.

5.3.3 And If *ApEn* Had Been Chosen?

At this point, once realized that the *SampEn* computation by segments reduces drastically the computation time, it is almost irresistible to also test *ApEn* statistics on real data in order to compare the results with the ones obtained with *SampEn*. Table 5.7 show the results for all the possible combinations of m and r, for CHF and healthy groups, and for methods of setting r.

Figure 5.4 shows the parameter combinations that achieve higher discrimination for each method of setting r. Note that these parameters are the same as the ones obtained for the *SampEn*.

The *ApEn* results and discrimination capabilities are very similar to the ones from the *SampEn*. The use of both statistics gives redundant information and none of them have proved

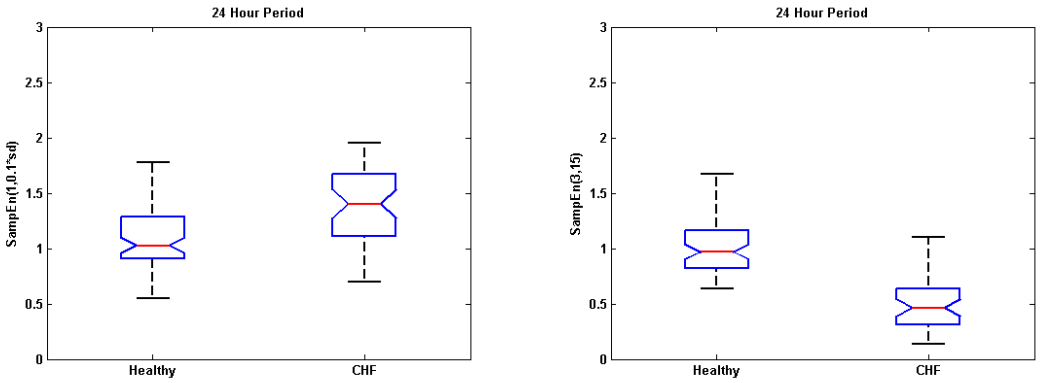

(a) (b)

Figure 5.3: *Boxplot for SampEn computed by segments over the 24 hour, for the healthy and the CHF groups. For r set by method 1 a). For r set by method 2 b).*

to largely outperform the other.

5.4 HRV Loss with Aging

In this section, first the discrimination capabilities of *SampEn* to distinguish between the young and the elderly groups are studied. Second, the recordings are split into six different groups according to the age of the subjects, and the evolution of the statistic is analyzed.

5.4.1 Discrimination Between Young and Elderly Subjects

The discrimination capabilities of the statistic to distinguish between young healthy and elderly healthy subjects are studied, by splitting the databases into two groups:

- Young group, from 20 to 50 years (26 recordings).
- Elderly group, from 51 to 80 years (46 recordings).

Table 5.8 shows the results for both methods of setting r and for all possible parameter combinations. Both methods provide higher values for young than for elderly subjects and similar discrimination capabilities between both groups. The reason is that the standard deviations from healthy young and healthy elderly groups are very similar (see 5.3), and therefore, in this case the standard deviation does not interfere in the computation of the irregularity degree when using method 1 for setting r.

Table 5.7: *Mean ± sd of ApEn computed by segments for both methods of setting r. All the available recordings are used. Significant variation between pathological and healthy subjects has been highlighted ($p < 0.05$ for r set by method 1 and $p < 10^{-11}$ for r set by method 2).*

$ApEn(m, rsd)$	CHF	Healthy	$ApEn(m, r)$	CHF	Healthy
$ApEn(3, 0.1sd)$	**1.01 ± 0.16**	**0.93 ± 0.15**	$ApEn(3, 10)$	**0.65 ± 0.22**	**0.97 ± 0.12**
$ApEn(2, 0.1sd)$	**1.30 ± 0.29**	**1.10 ± 0.24**	$ApEn(2, 10)$	**0.75 ± 0.27**	**1.18 ± 0.23**
$ApEn(1, 0.1sd)$	**1.53 ± 0.38**	**1.23 ± 0.29**	$ApEn(1, 10)$	**0.88 ± 0.29**	**1.33 ± 0.28**
$ApEn(3, 0.15sd)$	**0.84 ± 0.27**	**0.74 ± 0.22**	$ApEn(3, 15)$	**0.59 ± 0.25**	**0.97 ± 0.12**
$ApEn(2, 0.15sd)$	**1.00 ± 0.38**	**0.83 ± 0.28**	$ApEn(2, 15)$	**0.67 ± 0.30**	**1.18 ± 0.23**
$ApEn(1, 0.15sd)$	**1.16 ± 0.45**	**0.91 ± 0.30**	$ApEn(1, 15)$	**0.80 ± 0.32**	**1.33 ± 0.28**
$ApEn(3, 0.2sd)$	**0.77 ± 0.24**	**0.56 ± 0.17**	$ApEn(3, 20)$	**0.34 ± 0.21**	**0.73 ± 0.19**
$ApEn(2, 0.2sd)$	**0.79 ± 0.34**	**0.61 ± 0.22**	$ApEn(2, 20)$	**0.33 ± 0.17**	**0.82 ± 0.24**
$ApEn(1, 0.2sd)$	**0.91 ± 0.37**	**0.67 ± 0.23**	$ApEn(1, 20)$	**0.47 ± 0.25**	**0.89 ± 0.26**

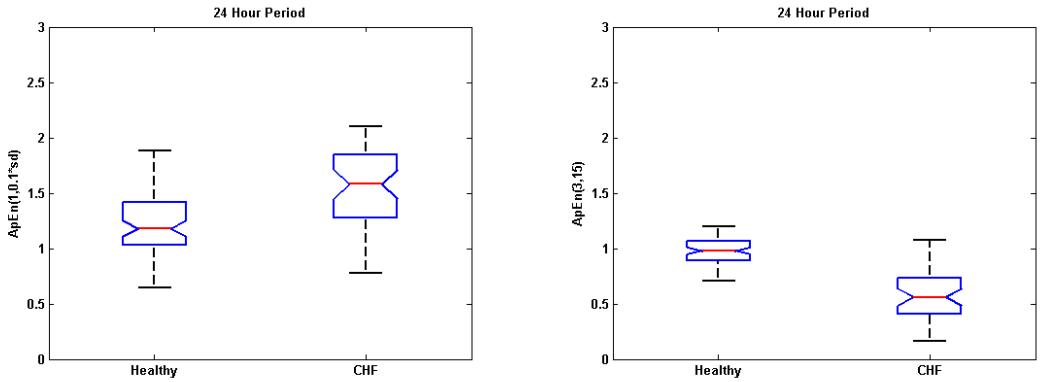

(a) (b)

Figure 5.4: *Boxplot for ApEn computed by segments over the 24 hour, for the healthy and the CHF groups. For r set by method 1 a). For r set by method 2 b).*

Table 5.8: *Mean ± sd of SampEn computed for young and elderly groups and for both methods of setting r. Significant variation ($p < 10^{-4}$) between pathological and healthy subjects has been highlighted.*

$SampEn(m, rsd)$	Young	Elderly	$SampEn(m, r)$	Young	Elderly
$SampEn(3, 0.10sd)$	**1.07 ± 0.19**	**0.82 ± 0.19**	$SampEn(3, 10)$	**1.16 ± 0.23**	**0.91 ± 0.17**
$SampEn(2, 0.10sd)$	**1.17 ± 0.22**	**0.88 ± 0.21**	$SampEn(2, 10)$	**1.27 ± 0.26**	**0.97 ± 0.19**
$SampEn(1, 0.10sd)$	**1.28 ± 0.24**	**0.98 ± 0.23**	$SampEn(1, 10)$	**1.38 ± 0.28**	**1.07 ± 0.20**
$SampEn(3, 0.15sd)$	**0.81 ± 0.21**	**0.57 ± 0.20**	$SampEn(3, 15)$	**1.16 ± 0.23**	**0.91 ± 0.17**
$SampEn(2, 0.15sd)$	**0.89 ± 0.24**	**0.62 ± 0.22**	$SampEn(2, 15)$	**1.27 ± 0.26**	**0.97 ± 0.19**
$SampEn(1, 0.10sd)$	**0.98 ± 0.25**	**0.70 ± 0.23**	$SampEn(1, 15)$	**1.38 ± 0.28**	**1.08 ± 0.20**
$SampEn(3, 0.20sd)$	**0.60 ± 0.15**	**0.40 ± 0.13**	$SampEn(3, 20)$	**0.80 ± 0.20**	**0.56 ± 0.14**
$SampEn(2, 0.20sd)$	**0.66 ± 0.18**	**0.43 ± 0.14**	$SampEn(2, 20)$	**0.87 ± 0.23**	**0.61 ± 0.13**
$SampEn(1, 0.20sd)$	**0.73 ± 0.19**	**0.50 ± 0.15**	$SampEn(1, 20)$	**0.95 ± 0.25**	**0.69 ± 0.17**

Figure 5.5 shows the parameter combination that achieves larger discrimination between young healthy and elderly healthy subjects for each method of setting r. These parameters are $m = 3$ for both methods, $r = 0.2sd$ for method 1 and $r = 20$ for method 2.

Figure 5.6 shows boxplots for young healthy, elderly healthy and CHF subjects for method 2 of setting r, and for the parameter combination that gives higher discrimination between healthy and pathological subjects (Fig 5.6 (a)); it also shows the parameter combination that gives higher discrimination between young and elderly subjects (Fig 5.6 (b)). For both cases $m = 3$, but the threshold r has a more stringent value for the second case: $r = 15$ and $r = 20$ respectively. These r values can be interpreted as if a thinner filter is necessary to differentiate between young and elderly subjects, than to differentiate between healthy and pathological subjects.

5.4.2 Aging Curve

As described above, both pathology and aging produce a HRV loss. It would be very helpful, if one could establish a *normal* loss of HRV due to aging in order to differentiate between this loss and the one caused by a pathology or any other disorder.

In this section the building of a possible aging curve is studied. For this purpose, the

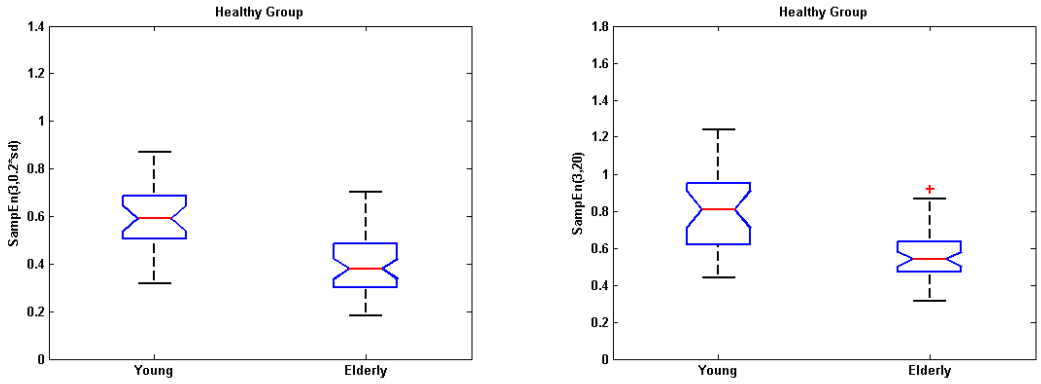

(a) (b)

Figure 5.5: *Boxplot for SampEn computed for young and elderly groups. For r set by method 1 a). For r set by method 2 b).*

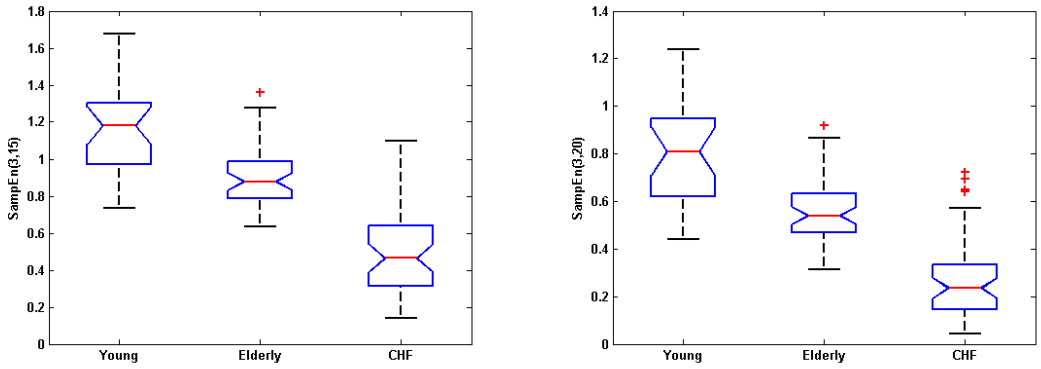

(a) (b)

Figure 5.6: *Boxplot for SampEn computed for young healthy, elderly healthy and CHF groups. For the parameter combination that gives higher discrimination between healthy and CHF groups a). For the parameter combination that gives higher discrimination between young and elderly groups b).*

Table 5.9: *SampEn evolution with age for the healthy group. Mean ± sd for both methods of setting r.*

Age(years)	$SampEn(2, 0.2sd)$	$SampEn(2, 20)$
20-30	0.61±0.13	0.91±0.29
31-40	0.68±0.21	0.86±0.21
41-50	0.63±0.20	0.76±0.24
51-60	0.58±0.07	0.67±0.16
61-70	0.42±0.14	0.61±0.15
71-80	0.47±0.16	0.54±0.20

recordings from the healthy subjects are divided into six different groups according to the age of the subjects, and *SampEn* is computed for each group in order to analyze the evolution of the statistic.

Table 5.9 and Figure 5.7 show the results for each age group and for both methods of setting r. With fixed r, it is possible to quantify the loss of HRV due to the aging in healthy subjects, which is less clearly present with variable r, since it does not show a steady increasing or decreasing tendency.

Following, the relation of the statistic with the age is analyzed using linear regression of the *SampEn* vs. age, and then obtaining the slope (variation vs. year index) and its determination coefficient, for both healthy and CHF groups.

Although linear regression shows significant variation for both methods of setting r ($p < 0.05$), the determination coefficient is higher for method 2.

The linear regression also shows that for CHF subjects no correlation is found between the age and the variation of *SampEn* results. An aging curve for CHF is not represented in this work since more recordings would be needed even for an initial study.

5.5 Normalized Entropies

In this section, normalized entropies are obtained for the healthy and CHF groups, as well as for the young and elderly groups. The aim of these experiments is to obtain a known maximum entropy value in order to allow a better comparison among the entropy values of the different

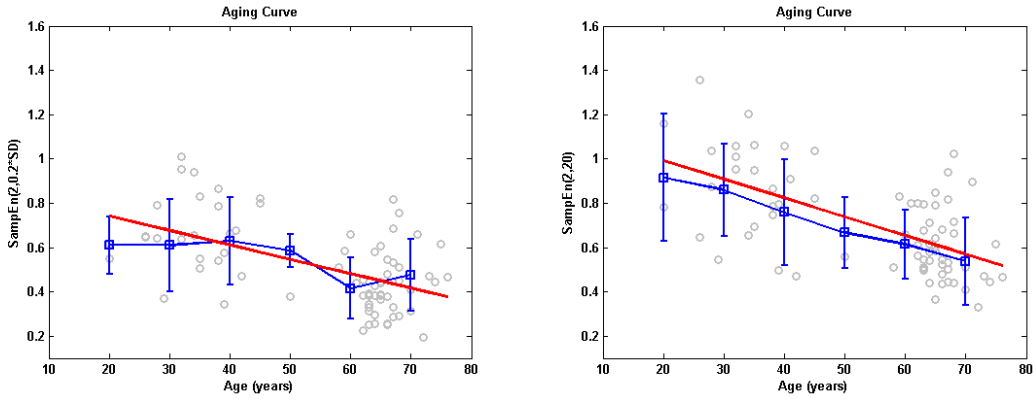

(a) (b)

Figure 5.7: *Evolution of SampEn with age for healthy subjects. Circles represent the SampEn for each subject, the squares the mean of each age group, the bars the standard deviation of each age group, and the straight line represents the fitted regression line. (a) For r as a percentage of each data series standard deviation. (b) For fixed r.*

Table 5.10: *Results of the linear regression of SampEn vs. age. Significant variation ($p < 0.05$) has been highlighted.*

		Index var/year	r^2
Healthy	$SampEn(2, 0.2sd)$	-0.0065	**0.2935**
	$SampEn(2, 20)$	-0.0085	**0.3653**
CHF	$SampEn(2, 0.2sd)$	-0.0125	0.1857
	$SampEn(2, 20)$	-0.0011	0.0036

Table 5.11: *Mean ± sd of normalized SampEn. Significant variation ($p < 0.05$) between healthy and pathological subjects has been highlighted.*

	$SampEn(3,0)$	$SampEn(2,0)$	$SampEn(1,0)$
Healthy	$\mathbf{0.31 \pm 0.12}$	$\mathbf{0.34 \pm 0.13}$	$\mathbf{0.40 \pm 0.13}$
CHF	$\mathbf{0.20 \pm 0.09}$	$\mathbf{0.25 \pm 0.10}$	$\mathbf{0.33 \pm 0.12}$

Table 5.12: *Mean ± sd of normalized SampEn. Significant variation ($p < 0.001$) between healthy and pathological subjects has been highlighted*

	$SampEn(3,0)$	$SampEn(2,0)$	$SampEn(1,0)$
Young	$\mathbf{0.40 \pm 0.12}$	$\mathbf{0.44 \pm 0.13}$	$\mathbf{0.48 \pm 0.14}$
Elderly	$\mathbf{0.26 \pm 0.08}$	$\mathbf{0.29 \pm 0.09}$	$\mathbf{0.15 \pm 0.03}$

groups.

To obtain these normalized results, first, the original time series must be normalized following the process explained in the example 3.2.1, therefore, 1 is now the maximum entropy value. Free parameters are set to, $m = 1, 2, 3$ and $r = 0$.

Tables 5.11 and 5.12 show the results for all possible parameter combinations. *SampEn(3,0)* achieves the larger discrimination between healthy and CHF groups and also between young and elderly subjects (Fig 5.8).

The discrimination capabilities of the normalized entropies are almost equal to the non-normalized ones between young and elderly groups. However, for the discrimination between healthy and CHF subjects, these capabilities are very inferior than the ones achieved with the non-normalized entropies, which is a limiting factor for using this approach.

5.6 *MSE* Analysis

In order to see if further relevant information can be obtained, related to the discrimination between healthy young, healthy elderly and CHF groups, an *MSE* analysis is performed with the real data.

Figure 5.9 (a) shows the *MSE* analysis for r set by method 1, the mean *SampEn* values are represented for each scale factor. The results are in agreement with the ones obtained

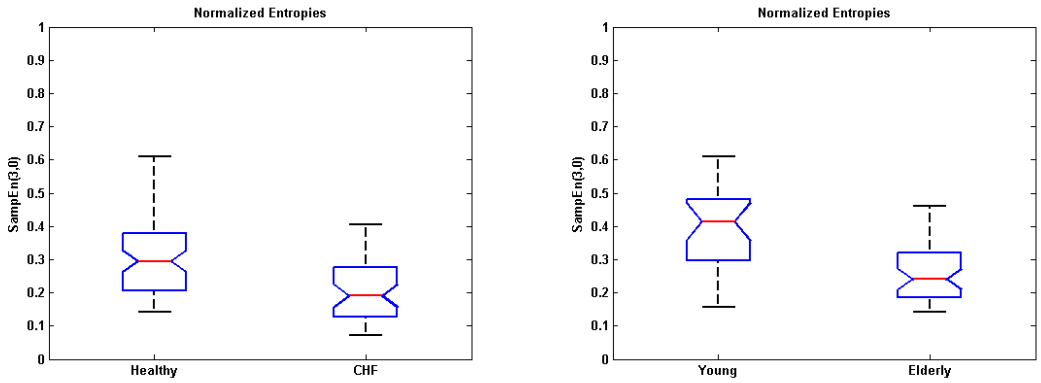

(a) (b)

Figure 5.8: *Box plot for normalized SampEn. For healthy and CHF groups a). For young and elderly groups b).*

in [Costa 03a]. For scale one, CHF subjects are assigned higher entropy values than healthy subjects, and time series of elderly healthy subjects are assigned the lowest entropy values. However, for all scales but the first one, healthy young subjects are assigned the highest entropy values. Although elderly healthy subjects only achieve higher entropy values than CHF subjects for a few scales.

Figure 5.9 (b) shows the *MSE* analysis for r set by method 2. The results show that similar discrimination between the groups is achieved, for all scale factors, and therefore the multiscale approach is unnecessary when a fixed threshold r is used.

5.7 Conclusion

In this chapter *SampEn* has been used to asses the variability of the RR-interval signals from 24-hour Holter recordings from healthy subjects and from patients suffering from CHF.

The experiments in this study have been divided in to two main parts; on one hand, the experiments that aim to discriminate between healthy and pathological subjects, and on the other hand, the experiments that study the relation of *SampEn* with aging.

From the first ones, the following conclusions can be extracted:

- The use of a fixed threshold value r, obtained as the mean standard deviation of the whole data set ensemble, instead of the more divulged use of r as a percentage of the standard deviation of each data series, produces better discrimination between healthy and CHF

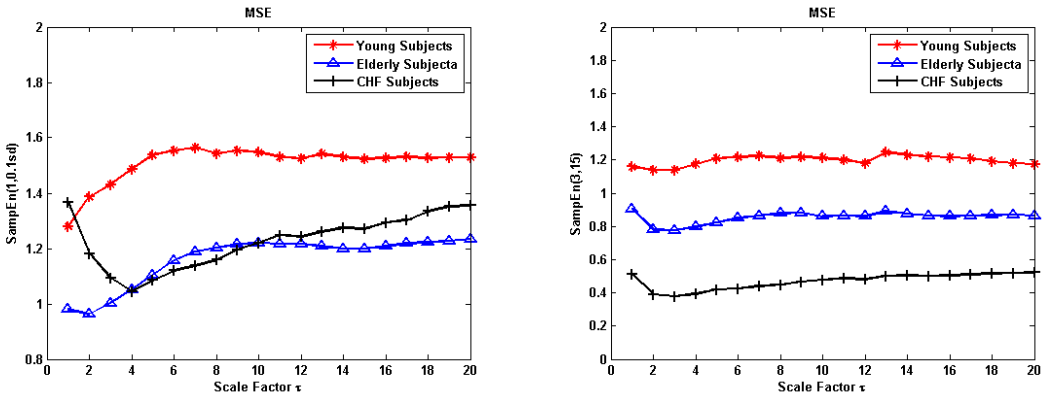

(a) (b)

Figure 5.9: *MSE analysis for healthy young subjects, healthy elderly subjects and CHF subjects. Symbols represent mean values for each scale factor. For r set by method 1 a). For r set by method 2 b).*

subjects. Also, higher *SampEn* values are obtained for healthy subjects than for CHF subjects, which is in agreement with the idea of loss of HRV in pathological conditions, whereas, for r set as a percentage of the standard deviation of each data series, higher *SampEn* values for CHF subjects than for healthy subjects are obtained.

- Computing *SampEn* by the proposed segments approach instead of doing it in a single step for the whole recording length, drastically reduces the computation time, maintaining the discriminating capabilities between healthy and pathological subjects.

- The results obtained from the study of the different time periods show that entropy values increase in the night period with respect to the day period. This could be attributed to the fact that during the day period, besides the complex physiological fluctuations that modulate the HR, other fluctuations with more regular patterns, which are the response to changes in the environmental conditions, are present, and this last fluctuations may disguise the irregularity inherent in the HRV signal.

- Largest discrimination between healthy and CHF subjects is achieved with the threshold value $r = 15$, that is, the 15% of the mean standard deviation of the whole data sets, for the three time periods, night, day and 24 hour. For the embeded dimension, $m = 3$ for the day and 24 hour periods, and $m = 2$ for the nigth period achieve the best results.

- *ApEn* statistics present similar results and discrimination capabilities to the ones from *SampEn*. The use of both statistics gives redundant information, and none of them have proved to largely outperform the other.

About the relation of *SampEn* with aging, the following conclusions can be drawn:

- Both methods of setting the threshold filter r provide higher entropy values for young than for elderly subjects, and they also present similar discrimination capabilities between both groups. The reason is that the standard deviations from healthy young and healthy elderly groups are very similar, and therefore, the standard deviation does not interfere in the computation of the irregularity degree when using method 1 for setting r.

- Free parameter combination $m = 3$, and $r = 20$ or $r = 0.2sd$, achieve the largest discrimination between the young and elderly groups.

- As expected, it is found that not only pathologies but also aging involves a loss of HRV.

- With a fixed threshold r, it is possible to quantify the loss of HRV due to aging in healthy subjects, which is less clearly present with variable r, since it does not show a fixed increasing or decreasing tendency.

- The performed linear regression shows that for CHF subjects no correlation is found between the age and the variation of *SampEn* results.

- Further studies with larger number of recordings are needed for the aim of building an usable aging curve of HRV loss for healthy subjects.

- An *MSE* analysis is unnecessary when a fixed threshold r is used, since similar discrimination is obtained, between healthy young, healthy elderly and CHF groups, for all the scale factors.

Chapter 6

Conclusions and Further Studies

In this work, a survey of the main HRV assessing methods has been presented, each one with different advantages and drawbacks. Among them, the signal entropy-based methods have been chosen in this work, for the good properties they present in the analysis of physiological signals.

Entropy-based methods stand up as a useful tool in the study of cardiac signals, and their possible application as a clinical tool for diagnosis or prediction of different cardiac pathologies has been widely explored [Magenes 03, Ferrario 06, Pincus 01, Marques-de Sá 05, Lake 02, Costa 02, Schuckers 99]. However, so far few attempts to introduce these applications on the clinical practice have been done, perhaps because there is not yet a clear consensus about the physiological meaning of the indices.

In this work, the three main entropy-based methods for the analysis of physiological signals have been presented and studied, namely, *ApEn*, *SampEn* and *MSE*. They were first tested in a controlled environment with well known synthetic signals, and then on real signals from both, healthy subjects and patients suffering from CHF.

The dependence of the algorithms on their free parameters and on the data length was tested, as well as the relative consistency of the methods. From the experiments performed on synthetic signals, it was concluded that although *SampEn* is sometimes not defined for extreme values of its free parameters, in the statistical valid range of these parameters, it achieves a better separation of processes with well known irregularity degrees than *ApEn*. Furthermore, it was found that *SampEn* agrees with theory in more situations, than *ApEn* does. However, it was also observed, the quite good performance of *ApEn* in the statistical valid range of its free parameters, which is the one used in the practice.

Due to the high computational cost of the algorithms for large data sets, *SampEn* was chosen, between both statistics, to perform the tests on RR-interval signals from 24-hour Holter recordings from healthy subjects and from patients suffering from CHF. By means of such tests, it was aimed to study the influence of the parameter tuning in the assessment of the HRV loss due to aging, and in the characterization of the HRV of patients affected by CHF, having in view a reliable discrimination between healthy and pathological subjects.

One of the most relevant findings was that the use of a fixed threshold value r, obtained as the mean standard deviation of the whole data sets, instead of the more widely popularized setting of r as a percentage of the standard deviation of each data series, yielded better discrimination between healthy and CHF subjects. Also, higher *SampEn* values were obtained for healthy subjects than for CHF subjects, which is in agreement with the idea of loss of HRV in pathological conditions, whereas, for r set as a percentage of the standard deviation of each data series, higher *SampEn* values for CHF subjects than for healthy subjects were obtained.

An approach of computing *SampEn* by segments over the 24 hour period instead of doing it in a single step for the whole recording length was proposed. This approach severely reduced the computation time, about 20 times less of computation time is needed, maintaining the discriminating capabilities.

Tests for different time periods of the day were performed, finding that entropy values increase in the night period with respect to the day period. This might be attributed to the fact that during the day period, besides the complex physiological fluctuations that modulate the HR, other fluctuations with more regular patterns, which are the response to changes in the environmental conditions, are present, and this last fluctuations may disguise the irregularity inherent in the HRV signal.

Once realized that the *SampEn* computation by segments drastically reduced the computation time, it was almost irresistible to also test *ApEn* statistics on real data in order to compare the results with the ones obtained with *SampEn*. The results showed similar discrimination capabilities than *SampEn* and none of them proved to largely outperform the other. Therefore, was verified that the use of both statistics gives redundant information.

The discrimination capabilities of the *SampEn* to distinguish between young and elderly groups of healthy subjects were also studied, and higher entropy values for young than for elderly subjects were obtained. Furthermore, a significant linear model explaining the variability decrease with age was derived.

Free parameter combination $m = 3$, and $r = 15$, achieved the largest discrimination between healthy and CHF groups, whereas, $m = 3$, and $r = 20$ achieved the largest discrimination between young and elderly groups, which can be seen as if a thinner filter is necessary to differentiate between young and elderly subjects, than to differentiate between healthy and pathological subjects.

Therefore and as expected, it was found that not only pathologies but also aging involves a loss of HRV, and it was an interesting finding that, with a fixed threshold r, it was possible to quantify the loss of HRV due to aging in healthy subjects which was not possible with variable r, since it did not show a fixed increasing or decreasing tendency. Moreover, no correlation was found for CHF subjects between the age and the variation of *SampEn* results.

MSE analysis were performed, and it was found that for r set as a percentage of each data series standard deviation, the results were in agreement with the ones found in the literature [Costa 03a], and showed better results for all the scales but the first one. However, when a fixed threshold r was used, similar discrimination capabilities were obtained for all scales, and therefore, the *MSE* analysis did not reveal further relevant information.

Further studies could derive from this work,

- First, the good discriminating capabilities that *SampEn* shows between healthy and CHF subjects could be tested for other cardiac pathologies that affect the HRV in order to have a more general tool for a possible clinical application.

- To implement a real clinical application, first, more intensive robustness tests should be performed. Also, the idea of combining *SampEn* with another index or indices, in order to enhance its discriminating capabilities seems interesting.

- Although promising results were found in the assessment of the HRV loss due to aging, further studies, with larger number of recordings are needed for the aim of building an usable aging curve of HRV loss for healthy subjects.

Appendices

Appendix A

MATLAB Functions

In this appendix the synthetic signals and the main functions implemented for the experiments in this work are presented.

A.1 MATLAB Function for *ApEn* Computation

```
function [res] = ApEn(X,r,m)
%"""""""""""""""""""""""""""""""""""""""""""""""""""""""""""""""""""""""""""""""
% PURPOSE:
% Function that estimates the aproximate entropy (ApEn) of a signal.
% USE:
% [res] = ApEn(X,r,m)
% ARGUMENTS...
% ...INPUT:
%       .-X ---> signal from which we want to compute ApEn.
%       .-r ---> noise filter threshold.
%       .-m ---> embedded dimension.
% ...OUTPUT:
%       .-res  ---> computed ApEn value.
%"""""""""""""""""""""""""""""""""""""""""""""""""""""""""""""""""""""""""""""""
X = X(:);
% ApEn final calculation.
```

```
res = Phym(m,r,X)-Phym(m+1,r,X);
%%%%%%%%%%%%%%%%%%%%%%%%%%%%%%%%%%%%%%%%%%%%%%%%%%%%%%%%%%%%%%%%%%%%%%%%%%%%
%Phy computation
function phym = Phym(m,r,X)
N = length(X);
% Matrix that contains all the template vectors to be compared to each other.
M = zeros(N-m+1,m);
[f,c] = size(M);
for i = 1:f
    M(i,:) = X(i:i+m-1);
end
% Computation of the correlation measure.
cm = zeros(f,1);
for i = 1:f
% Matrix whose rows are the template vectors to be compared with the rest of the
% vectors.
 Mi = repmat(M(i,:),f,1);
% For each row, the maximun of the columns from the differences matrix is obtained.
 dist = max(abs(Mi-M),[],2);
 cm(i) = length(find(dist<=r))/(N-m+1);
end
phym = mean(log(cm));
```

A.2 MATLAB Function for *SampEn* Computation

```
function [res] = SampEn(X,r,m)
%"""""""""""""""""""""""""""""""""""""""""""""""""""""""""""""""""""""""""""""""
% PURPOSE:
% Function that estimates the sample entropy (SampEn) of a signal.
% USE:
% [res] = SampEn(X,r,m)
% ARGUMENTS...
% ...INPUT:
%       .-X ---> signal from which we want to compute SampEn.
%       .-r ---> noise filter threshold.
%       .-m ---> embedded dimension.
% ...OUTPUT:
%       .-res  ---> computed SampEn value.
%"""""""""""""""""""""""""""""""""""""""""""""""""""""""""""""""""""""""""""""""
% Initial variables definition.
N = length(X);
X = X(:);
B_m_i = zeros(1,N-m);
A_m_i = zeros(1,N-m);
% Matrix that contains all the template vectors to be compared to each other.
for n = 1:2
M = zeros(N-m,m+n-1);
[f,c] = size(M);
for i = 1:f
   M(i,:) = X(i:i+m+n-2);
end
% Computation of the correlation measure.
for i = 1:f
   % Matrix whose rows are the template vectors to be compared with the rest of the
% vectors.
```

```
   Mi = repmat(M(i,:),f,1);
   % For each row, the maximun of the columns from the differences matrix is obtained.
   dist = max(abs(Mi-M),[],2);
   % To avoid selfmatches
   dist(i,:) = [];
   if n == 1
      B_m_i(i) = length(find(dist<=r))/(N-m-1);
   else
      A_m_i(i) = length(find(dist<=r))/(N-m-1);
   end
  end
end
B_m = mean(B_m_i);
A_m = mean(A_m_i);
% ApEn final calculation
res = log(B_m) - log(A_m);
```

A.3 MATLAB Function for *MSE* Computation

```
function  [entropies] = MSE(X,tau,r,m)
%"""""""""""""""""""""""""""""""""""""""""""""""""""""""""""""""""""""""""""""""
% PURPOSE:
% Function that estimates the multiscale entropy (MSE) of a signal.
% USE:
% [entropies] = MSE(X,tau,r,m)
% ARGUMENTS...
% ...INPUT:
%       .-X ---> signal from which we want to compute MSE.
%       .-r ---> noise filter threshold.
%       .-m ---> embedded dimension.
% .-tau ---> scale number.
% ...OUTPUT:
%       .-entropies  ---> computed MSE values.
%"""""""""""""""""""""""""""""""""""""""""""""""""""""""""""""""""""""""""""""""
X = X(:);
N = length(X);
% Coarse graining process
entropies = zeros(1,tau);
for  n = 1:tau
    y_tau=zeros(1,N/tau);
    for j = 1:N/n
    y_tau(j) =  mean(X(((j-1)*n+1):j*n));
    end
   % SampEn is computed for each coarse grained signal.
   entropies(n) = SampEn(y_tau,r,m);
end
```

A.4 MATLAB Function for Logistic Map

```
[logistic] = logisticMap(num,x0,a)
%"""""""""""""""""""""""""""""""""""""""""""""""""""""""""""""""""""""""""""""""
% PURPOSE:
% Function that generates a Logistic Map followin the equation:
% x(n+1)=ax(n)(1-x(n)).
% USE:
% [logistic] = logisticMap(num,x0,a)
% ARGUMENTS...
% ...INPUT:
%       .-num ---> number of points in the resulting signal.
%       .-x0 ---> initial value.
%       .-a ---> map parameter.
% ...OUTPUT:
%       .-logistic ---> output Logistic Map.
%"""""""""""""""""""""""""""""""""""""""""""""""""""""""""""""""""""""""""""""""
%Input variables validation
if nargin<3 | isempty(a)
% Default parameter value to obtain a cahotic behavior
    a = 3.8;
elseif ~isscalar(a)
    error('Parameter is not scalar');
end
if nargin<2 | isempty(x0)
    x0 = 0.1;
elseif ~isscalar(x0)
    error('The initial value must be scalar');
end
if nargin<1 | isempty(num)
    num = 5000;
```

```
elseif ~isscalar(num) | num<0
    error('Parameter must be scalar y positive.');
end
%%%%%%%%%%%%%%%%%%%%%%%%%%%%%%%%%%%%%%%%%%%%%%%%%%%%%%%%%%%%%%%%%%%%%%%%%%%%
%Map calculation
logistic = zeros(num,1);
%Initial value
logistic(1) = x0;
for m = 2:num
    logistic(m) = a*logistic(m-1)*(1-logistic(m-1));
end
```

A.5 MATLAB Function for MIX Processes

```
function [res] = MIX(n,p)
%"""""""""""""""""""""""""""""""""""""""""""""""""""""""""""""""""""""""""""""
% PURPOSE:
% Function that generates a MIX process, that is, a signal with both
% deterministic and stochastic components, each one to a greater or
% lesser extent depending on parameter p. For p=0, the signal will be
% completly deterministic and for p=1 the signal will be completly stochastic.
% USE:
% [res] = MIX(n,p)
% ARGUMENTS...
% ...INPUT:
%       .-n ---> number of points in the resulting signal.
%       .-p ---> parameter that controls the percentage of each signal
%                component.
%...OUTPUT:
%       .-res---> MIX process.
%"""""""""""""""""""""""""""""""""""""""""""""""""""""""""""""""""""""""""""""
%Deterministic component
X = sqrt(2)*sin((2*pi*(1:n))/12);
%Stochastic component
Y =  sqrt(3) + (-sqrt(3)-sqrt(3)) *rand(1,n);
Z  = zeros(1,n);
t=rand(1,n);
uno=find(t<p);
cero=find(t>p);
Z(uno) = 1;
Z(cero) = 0;
%Final MIX process
res = (1-Z).*X+Z.*Y;
```

A.6 MATLAB Function for AR Models

```
function [rrReposo,rrIncorporado,pxxR,fR,pxxI,fI]= ARmodelHRV(n)
%"""""""""""""""""""""""""""""""""""""""""""""""""""""""""""""""""""""""""""""""
% PURPOSE:
% Function that generates synthetic sequences which simulate HRV
% by adequate AR models.
% USE:
% [rrReposo,rrIncorporado,pxxR,fR,pxxI,fI] = ARmodelHRV(n);
% ARGUMENTS...
% ...INPUT:
%       .-n ---> number of points in the resulting sequences.
% ...OUTPUT:
%       .-rrReposo  ---> output sequence that simulates RR intervals for
%       a patient in rest.
%       .-rrIncorporado  --->output sequence that simulates RR intervals for
%       a patient in tilt.
% BIBLIOGRAFY:
%   .-Mateo, J. (1999). Anlisis espectral de la variabilidad del ritmo
%   cardaco mediante la seal de temporizacin cardaca. Departamento de
%   Ingeniera Electrnica y Comunicaciones. Zaragoza, Universidad de
%   Zaragoza.
%"""""""""""""""""""""""""""""""""""""""""""""""""""""""""""""""""""""""""""""""
% Input noise for the rest model.
ruidoR = wgn(1,n,db((404e-6)/2,'power'));
% Input noise for the tilt model.
ruidoI = wgn(1,n,db((137e-6)/2,'power'));
% Rest model parameters
aR = [1 -1.6265 1.8849 -1.8327 1.2970 -0.7758 0.4133 -0.2136];
% Rest model parameters
aI = [1 -1.8149 2.1365 -2.1703 1.7194 -0.9221 0.5311 -0.3262];
%Final synthetic signals
```

```
rrReposo = filter(1,aR,ruidoR);
rrIncorporado = filter(1,aI,ruidoI);
```

Bibliography

[Akselrod 81] S. Akselrod. *Power spectrum analysis of heart rate fluctuation: a quantitative probe of beat-to-beat cardiovascular control.* Science, vol. 213, pages 220–222, 1981.

[Association 08] American Heart Association. *Congestive Heart Failure.* `http://www.americanheart.org`, 2008.

[Barquero Pérez 05] O. Barquero Pérez. *Caos y Fractales en el Análisis de Variabilidad de Frecuencia Cardíaca.* Proyecto fin de carrera, Universidad Carlos III, 2005.

[Bigger 92] JT Bigger, JL Fleiss, RC Steinman, LM Rolnitzky, RE Kleiger & JN Rottman. *Frequency domain measures of heart period variability and mortality after myocardial infarction.* Circulation, vol. 85, no. 1, pages 164–171, 1992.

[Brennan 01] M. Brennan, M. Palaniswami & P. Kamen. *Do Existing Measures of Poincaré Plot Geometry Reflect Nonlinear Features of Heart Rate Variability?* IEEE Transactions on Biomedical Engineering, vol. 48, no. 11, pages 1342–1347, 2001.

[Cerutti 95] Sergio Cerutti, Anna M. Bianchi & Luca T. Mainardi. *Spectral Analysis of the Heart Rate Variability.* In Marek Malik & A. J. Camm, editors, Heart Rate Variability. Futura Publishing Company, New York, 1995.

[Costa 02] Madalena Costa, Ary L. Goldberger & C.-K. Peng. *Multiscale Entropy Analysis of Complex Physiologic Time Series.* Phys. Rev. Lett., vol. 89, no. 6, page 068102, 2002.

[Costa 03a] Madalena Costa & Healey J. A. *Multiscale Entropy Analysis of Complex Heart Rate Dynamics: Discrimination of Age and Heart Failure Effects.* Computers in Cardiology, vol. 30, pages 705–708, 2003.

[Costa 03b] Madalena Costa, C.-K. Peng, Ary L. Goldberger & Jeffre M. Hausdorff. *Multiscale entropy analysis of human gait dynamics.* Physica A, vol. 330, pages 53–60, 2003.

[Costa 05] Madalena Costa, Ary L. Goldberger & C.-K. Peng. *Multiscale entropy analysis of biological signals.* Phys. Rev. E, vol. 71, no. 2, page 021906, 2005.

[Cover 91] T M Cover & J A Thomas. Elements of information theory. Wiley, 1991.

[Eckmann 85] J P Eckmann & D Ruelle. *Ergodic Theory of chaos and strange attractors.* Reviews of modern physics, vol. 57, pages 617–656, 1985.

[Ferrario 06] Manuela Ferrario, Maria G. Signiorini, Giovanni Magenes & Sergio Cerruti. *Comparison of Entropy-Based Regularity Estimators: Application to the Fetal Heart Rate Signal for the Identification of Fetal Distress.* IEEE Transactions on biomedical engineering, vol. 53, no. 1, pages 119–125, 2006.

[Fogoros 03] Richard N. Fogoros. *Tilt Table Testing.* `http://heartdisease.about.com/cs/syncope/a/tilttabltesting.htm`, 2003.

[Goldberger 3] A. L. Goldberger, L. A. N. Amaral, L. Glass, J. M. Hausdorff, P. Ch. Ivanov, R. G. Mark, J. E. Mietus, G. B. Moody, C.-K. Peng & H. E. Stanley. *PhysioBank, PhysioToolkit, and PhysioNet: Components of a New Research Resource for Complex Physiologic Signals.* Circulation, vol. 101, no. 23, pages e215–e220, 2000 (June 13).

[Goldberger 91] Ari L. Goldberger. *Is the normal heartbeat chaotic or homeostatic?* New i. Phys. Sci., vol. 6, page 87, 1991.

[Goldberger 99] Ari L. Goldberger. *Nonlinear Dynamics, Fractals, and Chaos Theory: Implications for Neuroautonomic Heart Rate Control in health and disease.* http://www.physionet.org/tutorials/ndc, 1999.

[Grassberger 83] Peter Grassberger & Itamar Procaccia. *Estimation of the Kolmogorov entropy from a chaotic signal.* Physical Review A, vol. 28, pages 2591–2593, 1983.

[Guler 02] Inan Guler, Firat Hardala & Elif Derya Ubeyl. *Determination of Behcet disease with the application of FFT and AR methods.* Computers in Biology and Medicine, vol. 32, pages 419–434, 2002.

[Hornero 08] Roberto Hornero, Javier Escudero, Alberto Fernández, Jesús Poza & Carlos Gómez. *Spectral and Non-linear Analyses of MEG Background Activity in Patients with Alzheimer's Disease.* IEEE Transactions on biomedical engineering, vol. 55, no. 6, pages 1658–1665, 2008.

[Huikuri 99] Heikki V. Huikuri, Timo Makikallio, K. E. Juhani Airaksinen, Raul Mitrani, Agustin Castellanos & Robert J. Myerburg. *Measurement of Heart Rate Variability: A Clinical Tool or a Research Toy?* Journal of the American College of Cardiology, vol. 34, no. 7, pages 1878–1883, 1999.

[Huikuri 00] Heikki V. Huikuri, Timo Makikallio, C.K. Peng, Ary L. Goldberger, Ulrik Hintze & Mogens Moller. *Fractal correlation properties of RR interval dynamics and mortality in patients with depressed left ventricular function after an acute myocardial infarction.* Circulation, vol. 101, pages 47–53, 2000.

[Kantz 04] Holger Kantz & Thomas Schreiber. Nonlinear time series analysis. Cambridge University Press, 2004.

[Kaplan 95] Daniel Kaplan & Leon Glass. Understanding nonlinear dynamics. Springer, 1995.

[Lake 02] Douglas E. Lake, Joshua S. Richman, M. Pamela Griffin & J. Randall Moorman. *Sample entropy analysis of neonatal heart rate variability.* Am. J. Physiol. Heart. Circ. Physiol., vol. 283, pages 789–797, 2002.

[Lombardi 96] Federico Lombardi, Giulia Sandrone, Andrea Mortara, Daniela Torzillo, Maria Teresa La Rovere, Maria Gabriella Signorini, Sergio Cerutti & Alberto Malliani. *Linear and nonlinear dynamics of heart rate variability after acute myocardial infarction with normal and reduced left ventricular ejection fraction.* The American Journal of Cardiology, vol. 77, pages 1283–1288, 1996.

[Madera-Tejeda 02] R. Madera-Tejeda. *Análisis Comparativo de Medidas Espectrales de Potencia en la Señal de Variabilidad de Frecuencia Cardíaca.* Proyecto fin de carrera, Universidad de Alcalá, 2002.

[Magalhães 06] F. Magalhães, JP. Marques-de Sá, J. Bernardes & D. Ayres-de Campos. *Characterization of Fetal Heart Rate Irregularity Using Approximate Entropy and Wavelet Filtering.* IEEE. Computers in Cardiology, vol. 33, pages 933–936, 2006.

[Magenes 03] G. Magenes, M. G. Signorini, M. Ferrario, L. Pedrinazzi & D. Arduini. *Improving the fetal cardiotocographic monitoring by advanced signal processing.* Proc. IEEE EMBS, vol. 3, pages 2295–2298, 2003.

[Malik 89] Marek Malik, T. Farrell, T. Cripps & A. J. Camm. *Heart rate variability in relation to prognosis after myocardial infarction: Selection of optimal processing techniques.* European Heart Journal, vol. 10, pages 1060–1074, 1989.

[Malik 96] Marek Malik. *Heart rate variability. Standards of measurement, physiological interpretation, and clinical use.* European Heart Journal, vol. 17, pages 345–381, 1996.

[Marques-de Sá 05] Joaquim P. Marques-de Sá. *Characterization of Fetal Heart Rate Using Approximate Entropy.* IEEE. Computers in Cardiology, vol. 32, pages 671–673, 2005.

[Mateo 00] Javier Mateo. *Análisis espectral de la variabilidad del ritmo cardíaco mediante la seal de temporización cardíaca.* PhD thesis, Universidad de Zaragoza, 2000.

[Mietus 02] J E Mietus, C-K Peng, I Henry, R L Goldsmith & A L Goldberger. *The pNNx files: re-examining a widely used heart rate variability measure.* Heart, vol. 88, pages 378–380, 2002.

[Moody 06] George B. Moody. *Frequency Domain Measures: The Fourier Transform, the Lomb Periodogram, and Other Methods*, 2006.

[O. Rompelman 77] R. I. Kitney O. Rompelman A. J. R. M. Coenen. *Measurement of Heart Rate Variability.* MBEC, vol. 15, pages 233–239, 1977.

[Organization 08] World Health Organization. *Cardiovascular diseases.* `http://www.who.int/cardiovascular_diseases/en/`, 2008.

[Orstein 90] Donald S Orstein & Benjamin Weiss. *How Sampling Reveals a Process.* The Annals of Probability, vol. 18, pages 905–930, 1990.

[Persson 97] Pontus B. Persson. *Spectrum analysis of cardiovascular time series.* American Journal of Physiology - Regulatory Integrative Comparative Physiology, vol. 273, pages 1201–1210, 1997.

[Pincus 91] Steven M. Pincus. *Approximate entropy as a measure of system complexity.* Proc. Natl. Acad. Sci., vol. 88, pages 2297–2301, 1991.

[Pincus 92] Steven M. Pincus & Richard R. Viscarello. *Approximate Entropy: A Regularity Measure for Fetal Heart Rate Analysis.* Obstetrics and Ginecology, vol. 79, pages 249–255, 1992.

[Pincus 94] Steven M. Pincus & Ary L. Goldberger. *Physiological time-series analysis: what does regularity quantify?* Am. J. Physiol. Heart. Circ. Physiol., vol. 35, pages 1643–1656, 1994.

[Pincus 96] Steven M. Pincus & Burton H. Singer. *Randomness and degrees of irregularity.* Proc. Natl. Acad. Sci., vol. 93, pages 2083–2088, 1996.

[Pincus 01] Steven M. Pincus. *Assessing Serial Irregularity and Its Implications for Health.* Annals New York Academy of Sciences, vol. 954, pages 245–267, 2001.

[Piskorski 07] J. Piskorski & P. Guzik. *Geometry of the Poincaré plot of RR intervals and its asymmetry in healthy adults.* Physiological measurement, vol. 28, pages 287–300, 2007.

[Richman 00] Joshua S. Richman & J. Randall Moorman. *Physiological time-series analysis using approximate entropy and sample entropy.* Am. J. Physiol. Heart. Circ. Physiol., vol. 278, pages 2039–2049, 2000.

[Rojo-Álvarez 03] José Luis Rojo-Álvarez, Manel Martínez-Ramón, Aníbal R. Figueiras-Vidal, Ana García-Armada & Antonio Artés-Rodríguez. *A Robust Support Vector Algorithm for Nonparametric Spectral Analysis.* IEEE Signal Processing Letters, vol. 10, no. 11, pages 320–323, 2003.

[Sauner 07] Sauner. Dorland's medical dictionary for health consumers. Elsevier Academic Press, 2007.

[Schuckers 99] S A Caswell Schuckers & Pisut Raphisak. *Distinction of Arrhythmias with the Use of Approximate Entropy.* Computers in Cardiology, vol. 26, pages 347–350, 1999.

[Signiorini 94] Maria G. Signiorini & Sergio Cerutti. *Lyapunov exponents calculated from heart rate variability time series.* IEEE. Computers in Cardiology, vol. 1, pages 119–120, 1994.

[Signorini 98] Maria G. Signorini, Roberto Sassi, Federico Lombardi & Sergio Cerruti. *Regularity patterns in heart rate variability signal: the approximate entropy approach.* IEEE Proc. Eng. in Medicine and Biology Society, vol. 20, pages 306–309, 1998.

[Signorini 06] M. Signorini, M. Ferrario, M. Marchetti & A. Marseglia. *Nonlinear analysis of Heart Rate Variability signal for the characterization of Cardiac Heart Failure patients.* Conf Proc IEEE Eng Med Biol Soc, vol. 1, no. 1, pages 3431–3434, 2006.

[Sörnmo 05] Leif Sörnmo & Pablo Laguna. Bioelectrical signal processing in cardiac and neurological applications. Elsevier Academic Press, 1st edition, 2005.

[Yan 95] Xiangguo Yan & Chongxun Zheng. *Frequency-domain techniques for heart rate variability analysis.* IEEE-EMBC and CMBEC, vol. 2, pages 961–962, 1995.

[Zhang 91] Yi-Cheng Zhang. *Complexity and 1/f noise. A phase space approach.* Journal de physique I France, vol. 1, pages 971–977, 1991.